1 Outdoor and indoor ambient conditions

1.1 Overview

In building physics, the outdoor and indoor ambient conditions play a role comparable to the loads in structural engineering, which is why the term 'ambient loads' is often used. Their knowledge is essential to make correct design decisions. The components that shape them are:

Outdoors		Indoors	
Air temperature (also called dry bulb temperature)	θ_e	Air temperature (also called dry bulb temperature)	θ_i
		Radiant temperature	θ_R
Relative humidity	ϕ_e	Relative humidity	ϕ_i
(Partial water) vapour pressure	p_e	(Partial water) vapour pressure	p_i
Solar radiation	E_S		
Under-cooling	q_{rL}		
Wind	v_w	Air speed	v
Rain and snow	g_r		
Air pressure	$P_{a,e}$	Air pressure	$P_{a,i}$

In the paragraphs that follow, these components are discussed separately. Bear in mind though that the greater the decoupling between the outdoor and indoor temperatures, and sometimes the relative humidities, the stricter will be the envelope and HVAC performance requirements. Otherwise, much more energy will be needed to maintain those differences.

Predicting future outdoor conditions is hardly possible. Not only are most components measured in only a few locations but the future is never the same as the past. Unfortunately, climate does not obey the paradigm 'the longer the data chain available, the better the forecast'. Moreover, global warming is affecting everything, see Figure 1.1.

A typical way of bypassing the problem is by using reference values and reference years for each performance check that needs climate data, such as the heating and cooling load, end energy consumption, overheating, moisture tolerance and other durability issues.

Much of the data illustrating the facts and trends discussed in the following paragraphs comes from the weather station at Uccle, Belgium (50° 51′ north, 4° 21′ east). This is

Applied Building Physics: Ambient Conditions, Building Performance and Material Properties, Second Edition. Hugo Hens.

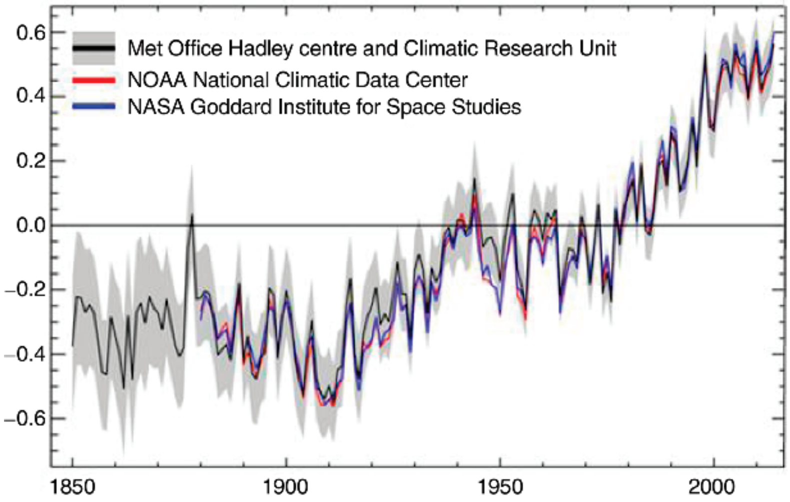

Figure 1.1 Increase in the world's average annual temperature between 1850 and 2014.

because of the large number of observations available, which allowed the synthesis of the weather there over the past century.

1.2 Outdoors

Geographical location defines, to a large extent, the outdoor climate: northern or southern latitude, proximity of the sea, presence of a warm or cold sea current and height above sea level. Of course, microclimatic factors also intervene. The urban heat island effect means that air temperature in city centres is higher, relative humidity lower and solar radiation less intense than in the countryside. Table 1.1 lists the monthly mean dry bulb temperature measured in a thermometer hut for the period 1901–1930 at Uccle and Sint Joost. Both weather stations are situated in the Brussels region, though the Uccle one overlooks a green area, while the Sint Joost one is in the city centre.

The outdoor climate further shows periodic fluctuations, linked to the earth's inclination and its elliptic orbit around the sun, the year and its succession of winter, spring, summer and autumn, and the wet and dry seasons in the equatorial band. Then there is the sequence of high and low pressure fronts; in temperate and cold climates, high brings

Table 1.1 Monthly mean dry bulb temperature at Uccle and Sint Joost, Brussels region, for the period 1901–1930 (°C).

Location	Month											
	J	F	M	A	M	J	J	A	S	O	N	D
Uccle	2.7	3.1	5.5	8.2	12.8	14.9	16.8	16.4	14.0	10.0	5.2	3.7
Sint Joost	3.8	4.2	6.8	9.4	14.6	16.7	18.7	18.0	15.4	11.2	6.4	4.7

warmth in summer and cold in winter, low gives cool and wet in summer and fresh and wet in winter. Finally, there is the effect of day and night, a consequence of the earth's rotation around its axis.

Design focuses on annual cycles, daily cycles and daily averages, but the meteorological references are 30-year averages, for the 20–21st century: 1901–1930, 1931–1960, 1961–1990, 1991–2020, 2021–2050 . . . These vary due to long-term climate changes as induced by solar activity and global warming, but the data is also affected by relocation of weather stations, more accurate measuring devices and the way averages are calculated. Up to 1930, the 'daily mean temperature' was the average of that day's minimum and maximum, as logged by a minimum/maximum mercury thermometer. Today, the air temperature at many weather stations is logged at 10′ intervals, and the daily mean is calculated as the average of these 144 values.

1.2.1 Air temperature

Knowing the air temperature helps in estimating the heating and cooling load and the related annual end energy consumption with the loads fixing the size and cost of the HVAC system needed and the end energy used being part of the annual costs. From day to day the air temperature also participates in the heat, air and moisture stresses that enclosures endure, while high values increase the indoor overheating risk. Measurement takes place in a thermometer hut in open field, 1.5 m above grade. The accuracy imposed by the World Meteorological Organization is ±0.5 °C. Table 1.2 covers over 30 years of averaged monthly means for several weather stations across Europe and North America. All look well represented by an annual mean and single harmonic, although adding a second harmonic gives a better fit:

Single harmonic

$$\theta_e = \overline{\theta}_e + A_{1,1}\sin\left(\frac{2\pi t}{365.25}\right) + B_{1,1}\cos\left(\frac{2\pi t}{365.25}\right) \tag{1.1}$$

Two harmonics

$$\begin{aligned}\theta_e = \overline{\theta}_e &+ A_{2,1}\sin\left(\frac{2\pi t}{365.25}\right) + B_{2,1}\cos\left(\frac{2\pi t}{365.25}\right)\\ &+ A_{2,2}\sin\left(\frac{4\pi t}{365.25}\right) + B_{2,2}\cos\left(\frac{4\pi t}{365.25}\right)\end{aligned} \tag{1.2}$$

In both formulas, $\overline{\theta}_e$ is the annual mean and t time. For three of the locations listed, the two-harmonic equation gives (°C, see Figure 1.2):

	$\overline{\theta}_e$	$A_{2,1}$	$B_{2,1}$	$A_{2,2}$	$B_{2,2}$
Uccle	9.8	−2.4	−7.4	0.45	−0.1
Kiruna	−1.2	−4.2	−11.6	1.2	0.5
Catania	17.2	−4.1	−6.6	0.8	0.2

Table 1.2 Monthly mean air temperatures for several locations (°C).

Location	Month											
	J	F	M	A	M	J	J	A	S	O	N	D
Uccle (B)	2.7	3.1	5.5	8.2	12.8	14.9	16.8	16.4	14.0	10.0	5.2	3.7
Den Bilt (NL)	1.3	2.4	4.3	8.1	12.1	15.3	16.1	16.1	14.2	10.7	5.5	1.2
Aberdeen (UK)	2.5	2.7	4.5	6.8	9.0	12.1	13.7	13.3	11.9	9.3	5.3	3.7
Eskdalemuir (UK)	1.8	1.9	3.9	5.8	8.9	11.8	13.1	12.9	10.9	8.5	4.3	2.7
Kew (UK)	4.7	4.8	6.8	9.0	12.6	15.6	17.5	17.1	14.8	11.6	7.5	5.6
Kiruna (S)	−12.2	−12.4	−8.9	−3.5	2.7	9.2	12.9	10.5	5.1	−1.5	−6.8	−10.1
Malmö (S)	−0.5	−0.7	1.4	6.0	11.0	15.0	17.2	16.7	13.5	8.9	4.9	2.0
Västerås (S)	−4.1	−4.1	−1.4	4.1	10.1	14.6	17.2	15.8	11.3	6.3	1.9	−1.0
Lulea (S)	−11.4	−10.0	−5.6	−0.1	6.1	12.8	15.3	13.6	8.2	2.9	−4.0	−8.9
Oslo (N)	−4.2	−4.1	−0.2	4.6	10.8	15.0	16.5	15.2	10.8	6.1	0.8	−2.6
München (D)	−1.5	−0.4	3.4	8.1	11.9	15.6	17.5	16.7	13.9	8.8	3.6	−0.2
Potsdam (D)	−0.7	−0.3	3.5	8.0	13.1	16.6	18.1	17.5	13.8	9.2	4.1	0.9
Roma (I)	7.6	9.0	11.3	13.9	18.0	22.3	25.2	24.7	21.5	16.8	12.1	8.9
Catania (I)	10.0	10.4	12.0	14.0	18.0	22.0	25.2	25.6	23.2	18.4	15.2	11.6
Torino (I)	1.6	3.5	7.6	10.8	15.4	19.0	22.3	21.6	17.9	12.3	6.2	2.4
Bratislava (Sk)	−2.0	0.0	4.3	9.6	14.2	17.8	19.3	18.9	15.3	10.0	4.2	0.1
Copenhagen (Dk)	−0.7	−0.8	1.8	5.7	11.1	15.1	16.2	16.0	12.7	9.0	4.7	1.1
Montreal	−9.9	−8.5	−2.4	5.7	13.1	18.4	21.1	19.5	14.6	8.5	1.8	−6.5
New York	0.6	2.2	6.1	11.7	17.2	22.2	25.0	24.4	20.0	13.9	8.9	3.3
Chicago	−5.6	−3.3	2.8	9.4	15.0	20.6	23.3	22.2	18.3	11.7	4.4	−2.8
Los Angeles	15.0	14.9	20.3	17.3	18.8	20.7	22.9	23.5	22.8	20.3	16.9	14.2

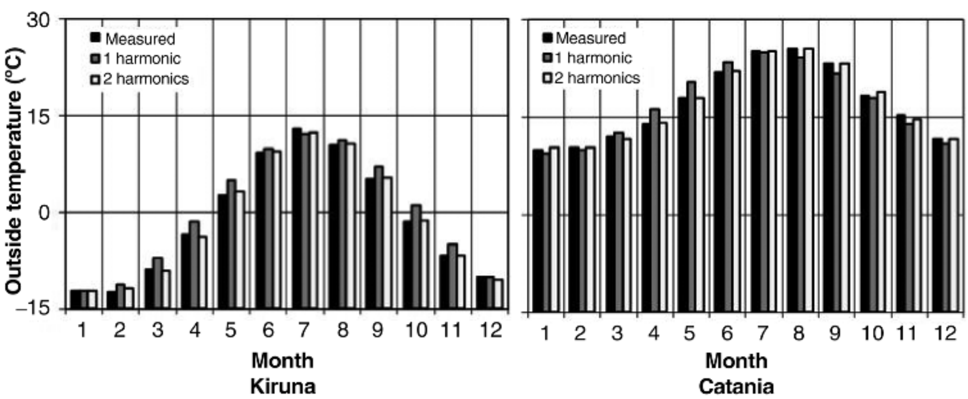

Figure 1.2 Air temperature: annual course, single and two harmonics.

For Uccle the average difference between the monthly mean daily minimums and maximums ($\theta_{e,max,day} - \theta_{e,min,day}$) during the period 1931 – 1960 looked as (°C):

J	F	M	A	M	J	J	A	S	O	N	D
5.6	6.6	7.9	9.3	10.7	10.8	10.6	10.1	9.8	8.0	6.2	5.2

A combination with the annual course could give (time in hours):

$$\begin{aligned}\theta_e &= \overline{\theta}_e + \hat{\theta}_e \cos\left[\frac{2\pi(t-h_1)}{8766}\right] \\ &\quad + \frac{1}{2}\left\{\Delta\overline{\theta}_{e,dag} + \Delta\hat{\theta}_{e,dag}\cos\left[\frac{2\pi(t-h_2)}{8766}\right]\right\}\sin\left[\frac{2\pi(t-h_3)}{24}\right]\end{aligned} \tag{1.3}$$

with:

$\Delta\overline{\theta}_{e,dag}$ (°C)	$\Delta\hat{\theta}_{e,dag}$ (°C)	h_1 (h)	h_2 (h)	h_3 (h)
8.4	2.8	456	−42	8

an equation, assuming that the daily values fluctuate harmonically. This is not the case. The gap between the daily minimum and maximum swings considerably, without even a hint of a harmonic course. To give an example, in Leuven, Belgium, that gap for January and July 1973 was purely random, with averages of 4.0 °C and 8.9 °C and standard deviation percentages 60 in January and 39 in July.

A question is whether the air temperature recorded during the past decades in any weather station reflects global warming? For that, the data recorded between 1997 and 2013 at the outskirts of Leuven were tabulated. Figure 1.3 shows the annual means and the monthly minima and maxima measured.

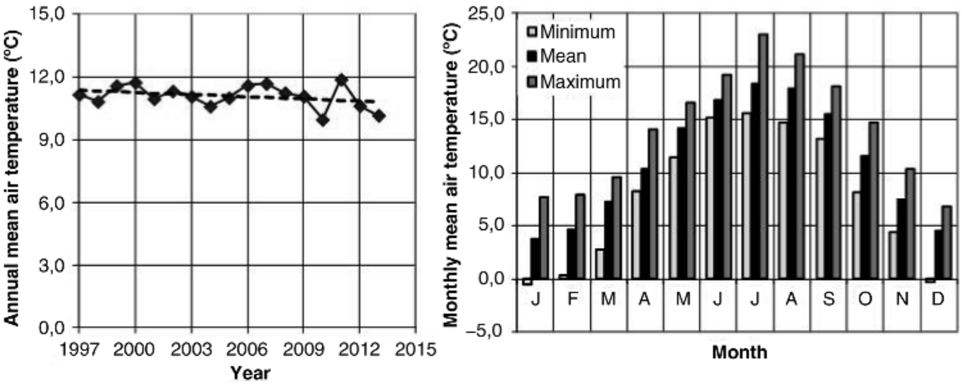

Figure 1.3 Leuven weather station (Belgium): air temperature between 1996 and 2013: annual mean (left) and average, minimum and maximum monthly mean (right).

The least square straight line through the annual means equals:

$$\overline{\theta}_{\mathrm{e,ann}} = 11.1 - 0.034 \times \mathrm{year}$$

With an of average 11.1 °C and a slightly negative slope, the expected increase seems absent. Not so at Uccle, 30 km west of Leuven. There the overall mean between 1901 and 1930 was 9.8 °C, that is 1.4 °C lower than measured at Leuven from 1997 to 2013. Between 1952 and 1971 that mean remained 9.8 °C but since then the moving 20-year mean has increased slowly, with the highest values noted between 1992 and 2011.

1.2.2 Solar radiation

Solar radiation means free heat gains. These lower the energy used for heating but may create cooling needs, as too many gains increase the overheating risk. The sun further lifts the outside surface temperature of irradiated envelope assemblies. Although this enhances drying, it also activates solar-driven vapour flow to the inside of moisture stored in rain buffering outer layers, whereas the associated drop in relative humidity aggravates hygrothermal stress in thin outer finishes.

The sun is a 5762 K hot black body, 150 000 000 km from the earth. Due to the large distance, the rays approach the earth in parallel. Above the atmosphere the solar spectrum follows the thin line in Figure 1.4, while the total irradiation is approximately:

$$E_{\mathrm{ST}} = 5.67\left(\frac{T_{\mathrm{S}}}{100}\right)^4\left(\frac{r_{\mathrm{S}}}{D_{\mathrm{SE}}}\right)^2 = 5.67\times(57.64)^4\times\left(\frac{0.695\cdot10^6}{1.496\cdot10^8}\right)^2 = 1332\,\mathrm{W/m^2} \quad (1.4)$$

with r_s the solar radius and D_{SE} the distance between sun and earth, both in km.

This 1332 W/m² represents the average solar constant (E_{STo}), that is the mean radiation per square metre that the earth would receive perpendicular to the beam if there were no atmosphere. The related energy flow is thinly spread. Burning 1 litre

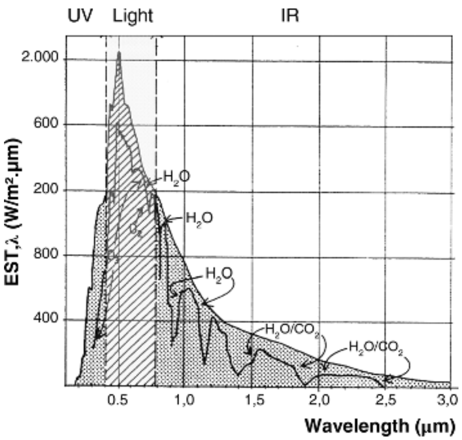

Figure 1.4 Solar spectrums before (thin) and after passing the atmosphere (thicker line).

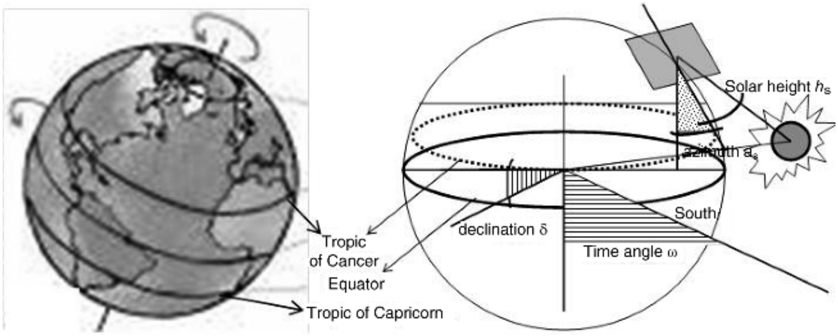

Figure 1.5 Solar angles.

of fuel gives 4.4×10^7 J, but collecting the same amount from the sun just above the atmosphere on a square metre perpendicular to the beam would take 9 hours of constant irradiation. This thinness explains why collecting solar energy for heat or electricity production requires such large surface areas. A more exact calculation of the solar constant accounts for the annual variation in distance between earth and sun and the annual cycle in solar activity (d the number of days from December 31/ January 1 at midnight):

$$E_{\text{STo}} = 1373\left\{1 + 0.03344\cos\left[\frac{2\pi}{365.25}(d - 2.75)\right]\right\}(\text{W/m}^2) \tag{1.5}$$

What fixes the solar position at the sky is either the azimuth (a_s) and solar height (h_s) or the time angle (ω) and declination (δ), that is the angle between the Tropics of Capricorn or Cancer, where the solar height reaches 90°, zenith position, and the equator plane, see Figure 1.5. The first two describe the sun's movement as seen locally, the second two relate it to the equator.

The time angle (ω) goes from 180° at 0 a.m. through 0° at noon to −180° at 12 p.m. One hour therefore corresponds to 15°. The declination (δ) in radians is given by:

$$\delta = arcsin\left[-\sin\left(\frac{\pi}{180}23.45\right)\cos\left[\frac{2\pi}{365.25}(d + 10)\right]\right] \tag{1.6}$$

where ±23.45 is the latitude of the Tropics in degrees. Solar height in radians at any moment equals:

$$h_s = \max\left[0, \pi/2 - \arccos(\cos\varphi\cos\delta\cos\omega + \sin\varphi\sin\delta)\right] \tag{1.7}$$

The maximum value ($h_{s,max}$) in degrees or radians follows from:

$$\text{Degrees}: h_{s.max} = 90 - \varphi(°) + \delta(°) \quad \text{Radians}: h_{s,max} = \pi/2 - \varphi + \delta \tag{1.8}$$

with φ latitude, positive for the northern, negative for the southern hemisphere. The addition (°) means values in degrees celsius.

1.2.2.1 Beam radiation

During its passage through the atmosphere, selective absorption by ozone, oxygen, hydrogen, carbon dioxide and methane interferes with the solar beam and changes its spectrum, while scattering disperses a part of it. The longer the distance traversed through the atmosphere, the more the radiation is affected, as represented by the air factor m, which is the ratio between the real distance traversed to sea level through the atmosphere, with the sun at height h_s and the distance traversed to any location at and above sea level, assuming that the sun stands in zenith position there (Figure 1.6).

For a location z km above sea level the air factor can be written as (all formulas below with solar height in radians):

$$m = \frac{L}{L_o} = \frac{1 - 0.1\,z}{\sin(h_s) + 0.15(h_s + 3.885)^{-1.253}} \tag{1.9}$$

Beam radiation on a surface perpendicular to the solar rays then becomes:

$$E_{SD,n} = E_{STo}\exp(-md_R T_{Atm})$$

where T_{Atm} is atmospheric turbidity and d_{R} the optic factor, a measure for the scatter per unit of distance traversed:

$$\begin{aligned} d_{\mathrm{R}} = {} & 1.4899 - 2.1099\cos(h_s) + 0.6322\cos(2h_s) + 0.0253\cos(3h_s) \\ & - 1.0022\sin(h_s) + 1.0077\sin(2h_s) - 0.2606\sin(3h_s) \end{aligned} \tag{1.10}$$

On a clear day with average air pollution, atmospheric turbidity is given by:

$$T_{\mathrm{Atm}} = 3.372 + 3.037h_s - 0.296\cos(0.5236\,\mathrm{mo})$$

With minimal air pollution, it becomes:

$$T_{\mathrm{Atm}} = 2.730 + 1.549\,h_s - 0.198\cos(0.5236\,\mathrm{mo})$$

In both formulas mo is the month, 1 for January, 12 for December.

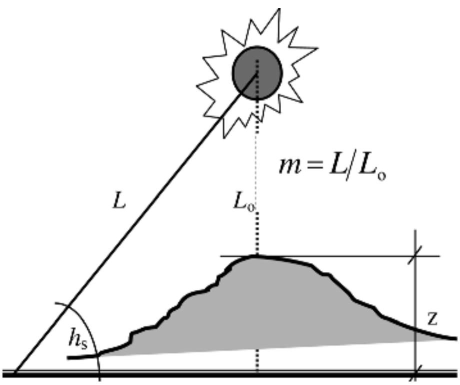

Figure 1.6 *L* the distance traversed through the atmosphere to sea level, *z* height of a location in km, L_o the distance traversed to *z* for the sun in zenith position.

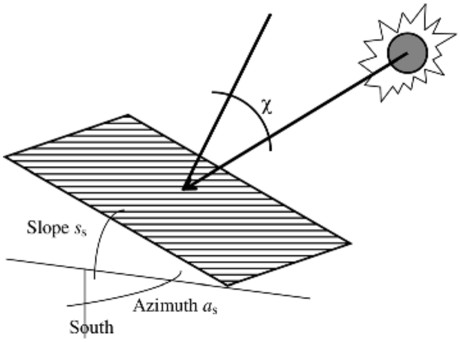

Figure 1.7 Direct radiation on a surface with slope s_s.

Beam radiation on a tilted surface, whose normal forms an angle χ with the solar rays, is calculated as (Figure 1.7):

$$E_{SD,s} = \max\left(0, E_{SD,n} \cos\chi\right) \tag{1.11}$$

with the zero to be applied before sunrise and after sunset and:

$$\begin{aligned}\cos\chi = {} & \sin\delta\sin\varphi\cos s_s - \sin\delta\cos\varphi\sin s_s\cos a_s \\ & + \cos\delta\cos\varphi\cos s_s\cos\omega + \cos\delta\sin\varphi\sin s_s\cos a_s\cos\omega \\ & + \cos\delta\sin s_s\sin a_s\sin\omega\end{aligned} \tag{1.12}$$

Here s_s is the surface's slope, 0° when horizontal, 90° ($\pi/2$) when vertical, between 0 and 90° when tilted to the sun, between 0 and −90° ($-\pi/2$) when tilted away from the sun, and a_s the surface's azimuth (south 0°, east 90°, north 180°, west −90°).

For a horizontal plane facing the sun the formula reduces to:

$$\cos\chi_h = \sin\delta\sin\varphi + \cos\delta\cos\varphi\cos\omega$$

For vertical planes facing the sun it becomes:

South $\cos\chi_{v,south} = -\sin\delta\cos\varphi + \cos\delta\sin\varphi\cos\omega$

West $\cos\chi_{v,west} = -\cos\delta\sin\omega$

North $\cos\chi_{v,north} = -\sin\delta\cos\varphi - \cos\delta\sin\varphi\cos\omega$

East $\cos\chi_{v,east} = \cos\delta\sin\omega$

Where the beam radiation on a horizontal surface is known ($E_{SD,h}$), its value on any tilted surface ($E_{SD,s}$) follows from:

$$E_{SD,s} = \max\left(0, E_{SD,h}\cos\chi_s/\cos\chi_h\right) \tag{1.13}$$

Beam radiation seems to be predictable, but the big unknown is the atmospheric turbidity (T_{Atm}). Cloudiness, air pollution and relative humidity all intervene, but their impact is very complex and varies from day to day.

1.2.2.2 Diffuse radiation

Whether the sky is blue or cloudy, diffuse solar radiation reaches the earth from sunrise to sunset. At the earth's surface, it's as if the rays come from all directions. The simplest model considers the sky as a uniformly radiating vault. Any surface, whose slope forms an angle with the horizontal, sees part of it. As a black body at constant temperature, each point on the vault has equal luminosity, turning the surface's view factor into:

$$F_{\mathrm{s,sk}} = (1 + \cos s_{\mathrm{s}})/2 \tag{1.14}$$

If $E_{\mathrm{Sd,h}}$ is the diffuse radiation on a horizontal surface, tilted it becomes:

$$E_{\mathrm{Sd,s}} = E_{\mathrm{Sd,h}}(1 + \cos s_{\mathrm{s}})/2 \tag{1.15}$$

Better approximating reality is the sky as a vault with the highest luminosity at the solar disk and the lowest at the horizon. With the position of any point P on that vault characterized by its azimuth a_{P} and height h_{P}, luminosity there writes as $L(a_{\mathrm{P}},h_{\mathrm{P}})$. The angle Γ between the normal on a surface with slope s_{s} and the line from its centre to this point P now equals:

$$\cos\Gamma = \sin s_{\mathrm{s}} \cos h_{\mathrm{P}} \cos(a_{\mathrm{s}} - a_{\mathrm{P}}) + \cos s_{\mathrm{s}} \sin h_{\mathrm{P}}$$

Diffuse radiation on a tilted surface therefore becomes:

$$E_{\mathrm{Sd,s}} = K_{\mathrm{D}} \iint\limits_{a_{\mathrm{P}},h_{\mathrm{P}}} \left[L_{a_{\mathrm{P}},h_{\mathrm{P}}} \cos h_{\mathrm{P}} \cos\Gamma\right] \mathrm{d}h_{\mathrm{P}}\mathrm{d}a_{\mathrm{P}} \tag{1.16}$$

with $K_{\mathrm{D}} = 1 + 0.03344\cos[0.017202(d - 2.75)]$, $0 \le a_{\mathrm{P}} \le 2\pi$, $0 \le h_{\mathrm{P}} \le \pi/2$, $\cos\Gamma \ge 0$ and:

$$L_{a_{\mathrm{P}},h_{\mathrm{P}}} = L_{\mathrm{sd}} \underbrace{\frac{\left[0.91 + 10\exp(-3\varepsilon) + 0.45\cos^2\varepsilon\right]\{1 - \exp[-0.32\,\mathrm{cosec}(h_{\mathrm{P}})]\}}{0.27385\left\{0.91 + 10\exp\left[-3\left(\frac{\pi}{2} - h_{\mathrm{S}}\right)\right] + 0.45\sin^2 h_{\mathrm{S}}\right\}}}_{f} \tag{1.17}$$

where L_{sd} is the luminosity at the solar disk and ε the angle between the line from the surface's centre to P and the normal on the vault in P, which coincides with the solar beam there:

$$\cos\varepsilon = \cos h_{\mathrm{S}} \cos h_{\mathrm{P}} \cos(a_{\mathrm{S}} - a_{\mathrm{P}}) + \sin h_{\mathrm{S}} \cos h_{\mathrm{P}}$$

Entering this formula and the multiplier from Eq. (1.17) in Eq. (1.16), results in:

$$E_{\mathrm{Sd,s}} = K_{\mathrm{D}} L_{\mathrm{zenith}} \iint\limits_{a_{\mathrm{P}},h_{\mathrm{P}}} [f \cos h_{\mathrm{P}} \cos\Gamma] \mathrm{d}h_{\mathrm{P}}\mathrm{d}a_{\mathrm{P}}$$

The luminosity at the solar disk then equals:

$$L_{\mathrm{sd}} = 0.8785[h_{\mathrm{s}}(°)] - 0.01322[h_{\mathrm{s}}(°)]^2 + 0.003434[h_{\mathrm{s}}(°)]^3 + 0.44347 + 0.0364 T_{\mathrm{Atm}}$$

Table 1.3 Uccle, multiplier f_{mo} for the total monthly diffuse radiation.

Azimuth → Slope ↓	0 S	22.5	45	67.5	90 E,W	112.5	135	157.5	180 N
0	1.00	1.00	1.00	1.00	1.00	1.00	1.00	1.00	1.00
22.5	1.03	1.03	1.02	1.01	1.00	0.99	0.98	0.97	0.96
45	1.05	1.04	1.03	1.01	0.99	0.96	0.94	0.92	0.92
67.5	1.06	1.05	1.03	0.99	0.94	0.90	0.86	0.84	0.83
90	1.06	1.04	1.00	0.94	0.87	0.81	0.76	0.73	0.71
112.5	0.98	0.97	0.92	0.85	0.76	0.68	0.63	0.60	0.60
135	0.80	0.78	0.74	0.67	0.59	0.53	0.49	0.47	0.47
157.5	0.58	0.56	0.51	0.48	0.46	0.43	0.41	0.40	0.34
180	0.00	0.00	0.00	0.00	0.00	0.00	0.00	0.00	0.00

with T_{Atm} atmospheric turbidity and $h_s(°)$ solar height in degrees. On a monthly basis, this set of formulas is simplified to:

$$E_{Sd,s} = E_{Sd,h} f_{mo}(1 + \cos s_s)/2$$

with f_{mo} a multiplier that corrects the monthly diffuse radiation, calculated according to (1.15) for the luminosity at the solar disk effect. For Uccle, f_{mo} takes the values given in Table 1.3.

1.2.2.3 Reflected radiation

Surfaces on earth reflect part of the beam and diffuse radiation received. To calculate the intensity, all surroundings are considered to be acting as one horizontal plane with reflectivity 0.2, called the albedo. Every surface then receives reflected radiation proportional to the view factor with that horizontal plane (F_{se}):

$$E_{Sr,s} = 0.2\left(E_{SD,h} + E_{Sd,h}\right)F_{se} = 0.2\left(E_{SD,h} + E_{Sd,h}\right)(1 - \cos s_s)/2 \tag{1.18}$$

Reflected radiation on a horizontal surface facing the sky ($s_s = 0$) looks to be zero though in reality this is not by definition the case. A low-sloped roof for example gets radiation reflected from surrounding higher buildings. Also, an albedo of 0.2 is too simplistic. White snow gives a higher value.

1.2.2.4 Total radiation

Beam, diffuse and reflected irradiation together give the total solar radiation that a surface receives. The appendix contains tables with values for Uccle, while Table 1.4 here summarizes the average, minimum and maximum monthly totals on a horizontal surface measured there, together with the monthly mean cloudiness, calculated as one minus the ratio between the measured and clear sky total on a horizontal surface. Table 1.5 in turn lists the monthly totals on a horizontal surface for several locations

Table 1.4 Monthly total solar irradiation on a horizontal surface (MJ/(m^2.month)) and cloudiness at Uccle, average, maximum and minimum values for 1958–1975.

	J	F	M	A	M	J	J	A	S	O	N	D
Total solar radiation												
Mean	72	129	247	356	500	538	510	439	327	197	85	56
Min.	61	104	177	263	406	431	408	366	279	145	63	41
Max.	93	188	311	485	589	640	651	497	444	274	112	78
Average cloudiness												
Mean	0.47	0.44	0.42	0.42	0.36	0.35	0.38	0.38	0.34	0.39	0.49	0.50
Min.	0.55	0.55	0.58	0.57	0.48	0.48	0.51	0.48	0.44	0.55	0.62	0.63
Max.	0.31	0.19	0.27	0.20	0.25	0.22	0.21	0.30	0.11	0.15	0.33	0.30

across Europe, while Figure 1.8 shows the annual totals with the ratio between least and most sunny location approaching a value of 2.

How sunny locations are is important when questions are raised such as where to promote photovoltaic cells (PV) as renewable. Within Europe, PV is good in Portugal, Spain, Southern France, Southern Italy and Greece, but of only moderate benefit in the north-west and Scandinavia.

1.2.3 Longwave radiation

Longwave radiation gives extra heat loss as it can chill the outer surface and the layers outside of the insulation to temperatures below those of outdoors, even below the dew point outdoors. Under-cooling, as it is called, turns the outdoor air into a moisture source rather

Table 1.5 Monthly total solar irradiation on a horizontal surface for several locations in Europe (MJ/(m^2.month)).

Location	Month											
	J	F	M	A	M	J	J	A	S	O	N	D
Den Bilt (NL)	72	132	249	381	522	555	509	458	316	193	86	56
Eskdalemuir (UK)	55	112	209	345	458	490	445	370	244	143	70	39
Kew (UK)	67	115	244	355	496	516	501	434	311	182	88	54
Lulea (S)	6	52	182	358	528	612	589	418	211	80	14	1
Oslo (N)	44	110	268	441	616	689	624	490	391	153	57	27
Potsdam (D)	104	137	238	332	498	557	562	412	267	174	88	70
Roma (I)	182	247	404	521	670	700	750	654	498	343	205	166
Torino (I)	171	212	343	474	538	573	621	579	422	281	181	148
Bratislava (Sk)	94	159	300	464	597	635	624	544	389	233	101	72
Copenhagen (Dk)	54	114	244	407	579	622	576	479	308	159	67	38

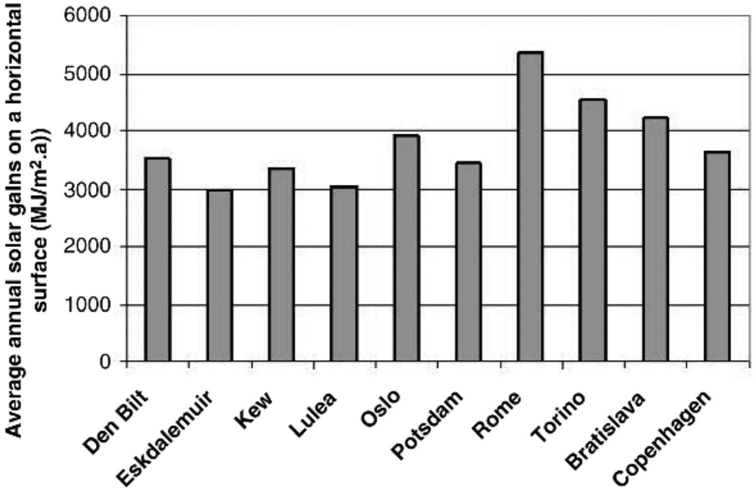

Figure 1.8 Annual solar radiation on a horizontal surface.

than a drying medium with a visible result being condensation on the outer surface of insulating glass, EIFS-stucco and tiled or slated well-insulated pitched roofs (Figure 1.9).

Under-cooling reflects the longwave balance between the atmosphere, represented by the celestial vault, the terrestrial plane and the surface considered, with the vault acting as a selective radiant body, absorbing all incoming radiation but emitting only a fraction. Calculation assumes a vault at air temperature with emissivity below 1, absorptivity 1 and reflectivity 0. Several formulas quantify its emissivity. To give a few (p_e in Pa, θ_e in °C):

Clear sky

(1) $\varepsilon_{L,sky,o} = 0.75 - 0.32 \cdot 10^{-0.051 p_e/1000}$

(2) $\varepsilon_{L,sky,o} = 0.52 + 0.065\sqrt{p_e/1000}$

(3) $\varepsilon_{L,sky,o} = 1.24\left(\dfrac{p_e/1000}{273.15 + \theta_e}\right)^{1/7}$

Cloudy sky

(4) $\varepsilon_{L,sky} = \varepsilon_{L,sky,o}(1 - 0.84c) + 0.84c$

Figure 1.9 Rime formation on a well-insulated pitched roof due to under-cooling.

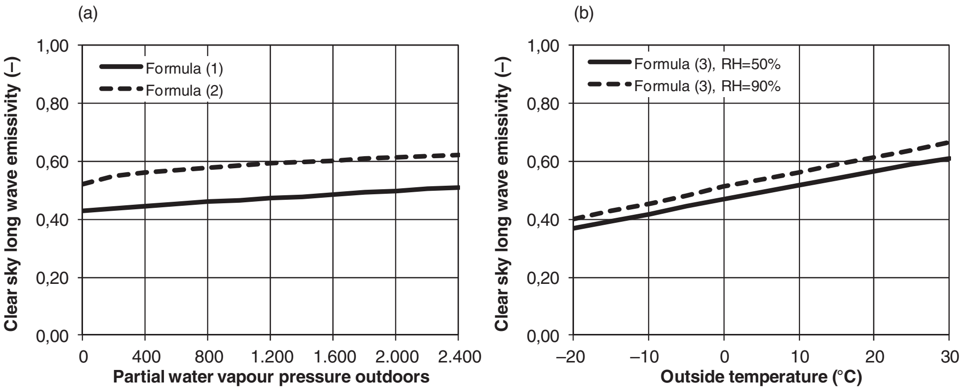

Figure 1.10 Sky emissivity, left according to the clear sky formulas (1) and (2), right according to the clear sky formula (3).

Clear sky emissivity thus drops with air temperature but increases with partial water vapour pressure outdoors as water vapour in fact acts as a strong greenhouse gas. In the cloudy sky formula, c stands for the cloudiness factor, 0 for clear, steps 0.125 for hardly covered to more covered and 1 for a covered sky. According to Figure 1.10(a) left, the formulas (1) and (2) apparently give a different emissivity, whereas Figure 1.10(b), illustrating formula (3), suggests that (1) applies to lower and (2) to somewhat higher temperatures outdoors.

The following two equations for the black body emittance of the surface considered and the terrestrial plane describe the 'celestial vault/surface/terrestrial plane' radiant system:

$$M_{\mathrm{b,s}} = \left[1 + \frac{\rho_{\mathrm{L,s}}}{\varepsilon_{\mathrm{L,s}}}\left(F_{\mathrm{s,t}} + F_{\mathrm{s,sky}}\right)\right]M'_{\mathrm{s}} - \frac{\rho_{\mathrm{L,s}}}{\varepsilon_{\mathrm{L,s}}}\left(F_{\mathrm{s,t}}M'_{\mathrm{t}} + F_{\mathrm{s,sky}}M'_{\mathrm{sky}}\right)$$

$$M_{\mathrm{b,t}} = \left[1 + \frac{\rho_{\mathrm{L,t}}}{\varepsilon_{\mathrm{L,t}}}\left(F_{\mathrm{t,s}} + F_{\mathrm{t,sky}}\right)\right]M'_{\mathrm{t}} - \frac{\rho_{\mathrm{L,t}}}{\varepsilon_{\mathrm{L,t}}}\left(F_{\mathrm{t,s}}M'_{\mathrm{s}} + F_{\mathrm{t,sky}}M'_{\mathrm{sky}}\right)$$

In both, the suffix s stands for the surface, the suffix t for the terrestrial plane, the suffix sky for the celestial vault, M'_{sky} for the radiosity of the celestial vault and $F_{\mathrm{s,t}}$, $F_{\mathrm{s,sky}}$, . . . for the view factors between these radiant bodies. As that plane and celestial vault surround the surface, the sum $F_{\mathrm{s,t}} + F_{\mathrm{s,sky}}$ is 1. The same holds for the view factor between the terrestrial plane and the celestial vault. In fact, the one between that plane and the surface is so small that using zero does not falsify the second equation. Celestial vault radiosity thus simplifies to:

$$M'_{\mathrm{sky}} = \varepsilon_{\mathrm{L,sky}} M_{\mathrm{b,sky},\theta_{\mathrm{e}}}$$

turning the two equations into:

$$M_{\mathrm{b,s}} = \frac{1}{\varepsilon_{\mathrm{L,s}}}M'_{\mathrm{s}} - \frac{\rho_{\mathrm{L,s}}}{\varepsilon_{\mathrm{L,s}}}\left(F_{\mathrm{s,t}}M'_{\mathrm{t}} + F_{\mathrm{s,sky}}\varepsilon_{\mathrm{L,sky}}M_{\mathrm{b,sky},\theta_{\mathrm{e}}}\right) \tag{1.19}$$

$$M_{\mathrm{b,t}} = \frac{1}{\varepsilon_{\mathrm{L,t}}}\left(M'_{\mathrm{t}} - \rho_{\mathrm{L,t}}\varepsilon_{\mathrm{L,sky}}M_{\mathrm{b,sky},\theta_{\mathrm{e}}}\right) \tag{1.20}$$

The radiant heat flow rate at the surface is now:

$$q_{\mathrm{R}} = q_{\mathrm{Rs,t}} + q_{\mathrm{Rs,sky}} = \frac{\varepsilon_{\mathrm{L,s}}}{\rho_{\mathrm{L,s}}}\left(M_{\mathrm{b,s}} - M'_{\mathrm{s}}\right) = \varepsilon_{\mathrm{L,s}} F_{\mathrm{s,t}}\left(M_{\mathrm{b,s}} - \varepsilon_{\mathrm{L,t}} M_{\mathrm{b,t}}\right) + \varepsilon_{\mathrm{L,s}} F_{\mathrm{s,sky}}\left[M_{\mathrm{b,s}} - \left(\rho_{\mathrm{L,env}}\frac{F_{\mathrm{s,t}}}{F_{\mathrm{s,t}}} + 1\right)\varepsilon_{\mathrm{L,sky}} M_{\mathrm{b,sky},\theta_{\mathrm{e}}}\right]$$

Assuming the terrestrial plane to be a black body at outdoor air temperature further simplifies the formula:

$$q_{\mathrm{R}} = \varepsilon_{\mathrm{L,s}} C_{\mathrm{b}}\left[\left(F_{\mathrm{s,t}} + F_{\mathrm{s,sky}}\right)\left(\frac{T_{\mathrm{se}}}{100}\right)^4 - \left(F_{\mathrm{s,t}} + F_{\mathrm{s,sky}}\varepsilon_{\mathrm{L,sky}}\right)\left(\frac{T_{\mathrm{e}}}{100}\right)^4\right] \tag{1.21}$$

Linearization by replacing the celestial vault by a black body at temperature

$$\theta_{\mathrm{sk,e}} = \theta_{\mathrm{e}} - (23.8 - 0.2025\,\theta_{\mathrm{e}})(1 - 0.87c)$$

gives:

$$q_{\mathrm{R}} = \varepsilon_{\mathrm{L,s}} C_{\mathrm{b}}\left[\begin{array}{l}\left(F_{\mathrm{s,t}} F_{\mathrm{Ts,t}} + F_{\mathrm{s,sky}} F_{\mathrm{Ts,sky}}\right)(\theta_{\mathrm{se}} - \theta_{\mathrm{e}}) \\ \qquad + (23.8 - 0.2025\,\theta_{\mathrm{e}})(1 - 0.87c) F_{\mathrm{s,sky}} F_{\mathrm{Ts,sky}}\end{array}\right] \tag{1.22}$$

a result that fits with expression (1.21) for a sky emissivity somewhat higher than in Figure 1.10(b). Combining (1.22) with the convective heat exchanged quantifies under-cooling:

$$\begin{aligned} q_{\mathrm{ce}} + q_{\mathrm{Re}} = &\left[h_{\mathrm{ce}} + \varepsilon_{\mathrm{L,s}} C_{\mathrm{b}}\left(F_{\mathrm{s,t}} F_{\mathrm{Ts,t}} + F_{\mathrm{s,sky}} F_{\mathrm{Ts,sky}}\right)\right](\theta_{\mathrm{se}} - \theta_{\mathrm{e}}) \\ &+ \varepsilon_{\mathrm{L,s}} C_{\mathrm{b}} F_{\mathrm{s,sky}} F_{\mathrm{Ts,sky}}(23.8 - 0.2025\,\theta_{\mathrm{e}})(1 - 0.87c) \end{aligned} \tag{1.23}$$

$$q_{\mathrm{T}} + q_{\mathrm{ce}} + q_{\mathrm{Re}} = 0$$

where q_{T} is the heat flow rate by transmission to or from the exterior surface. Figure 1.11 shows calculated data for a low-slope roof with thermal transmittance 0.2 W/(m^2.K),

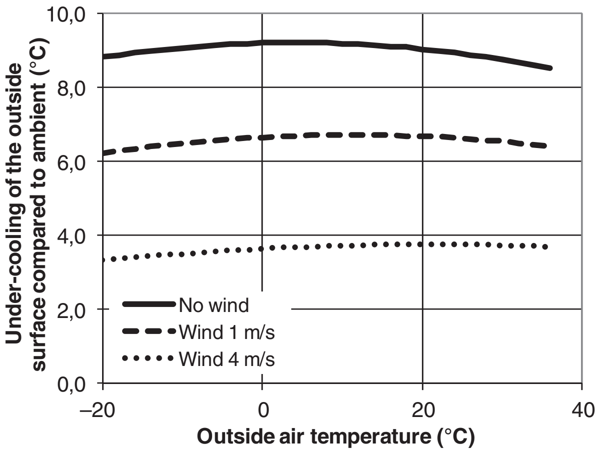

Figure 1.11 Lightweight low-sloped roof, U = 0.2 W/(m^2.K), membrane with $e_{\mathrm{L}} = 0.9$: under-cooling represented by $\theta_{\mathrm{e}} - \theta_{\mathrm{se}}$.

a membrane with longwave emissivity 0.9 and very low thermal inertia. Parameters are the air temperature and wind speed. The outside surface temperature can drop substantially below ambient.

1.2.4 Relative humidity and (partial water) vapour pressure

Both relative humidity (ϕ_e) and (partial water) vapour pressure (p_e) impact the moisture tolerance of building enclosures and buildings in a straightforward way. Table 1.6 summarizes monthly means for several locations across Europe.

On average, relative humidity hardly changes between winter and summer. Vapour pressure, however, does. In temperate climates the inverse often holds between day and night: large differences in relative humidity and fairly constant vapour pressures. A sudden temperature rise lowers the relative humidity while a sudden drop may push it up to a misty 100%. During rainy weather the wet bulb temperature closely follows the raindrop temperature. When it is as warm as the air, relative humidity will near 100%. Also, the environment strongly influences relative humidity and vapour pressure, with higher values in forests and river valleys than in cities. Again, the annual variation is often written in terms of a Fourier series with one harmonic, though, as Figure 1.12

Table 1.6 Monthly mean relative humidity (%) and vapour pressure (Pa, bold) for several locations all over Europe.

Location	Month											
	J	F	M	A	M	J	J	A	S	O	N	D
Uccle (B)	89.6	89.0	84.0	78.5	77.8	78.9	79.9	79.8	84.2	88.3	91.2	92.7
	663	**681**	**757**	**854**	**1151**	**1334**	**1529**	**1489**	**1346**	**1084**	**806**	**780**
Aberdeen (UK)	81.5	80.3	74.9	72.3	75.0	78.5	74.1	79.1	80.6	81.6	78.1	77.1
	596	**596**	**631**	**714**	**860**	**1107**	**1161**	**1207**	**1122**	**955**	**695**	**614**
Catania (I)	66.5	72.4	68.8	69.8	71.2	70.0	62.0	68.6	69.4	69.6	68.5	65.9
	816	**912**	**964**	**1114**	**1469**	**1849**	**1985**	**2252**	**1972**	**1471**	**1183**	**900**
Den Bilt (NL)	86.1	82.1	76.0	75.9	72.9	72.7	77.1	78.9	80.7	84.4	85.5	86.8
	578	**596**	**631**	**811**	**1028**	**1263**	**1411**	**1443**	**1306**	**1086**	**772**	**587**
Kiruna (S)	83.0	82.0	77.0	71.0	64.0	61.0	68.0	72.0	77.0	81.0	85.0	85.0
	177	**171**	**221**	**324**	**476**	**710**	**1011**	**914**	**676**	**436**	**292**	**219**
Malmö (S)	87.0	86.0	83.0	76.0	73.0	74.0	78.0	77.0	82.0	85.0	87.0	89.0
	510	**496**	**561**	**711**	**958**	**1262**	**1531**	**1464**	**1269**	**969**	**753**	**627**
Munich (G)	83.7	81.9	76.8	72.3	74.9	76.8	74.2	76.1	79.2	82.9	83.5	85.7
	451	**484**	**598**	**780**	**1043**	**1361**	**1483**	**1446**	**1267**	**938**	**660**	**515**
Rome (I)	76.1	71.3	66.5	69.1	71.4	71.3	61.6	68.5	72.3	74.1	78.1	79.4
	794	**764**	**816**	**1048**	**1400**	**1795**	**1881**	**2042**	**1776**	**1346**	**1124**	**874**
Västerås (S)	84.0	82.0	74.0	66.0	62.0	65.0	69.0	74.0	81.0	83.0	86.0	86.0
	364	**355**	**402**	**540**	**766**	**1081**	**1354**	**1328**	**1085**	**793**	**602**	**483**

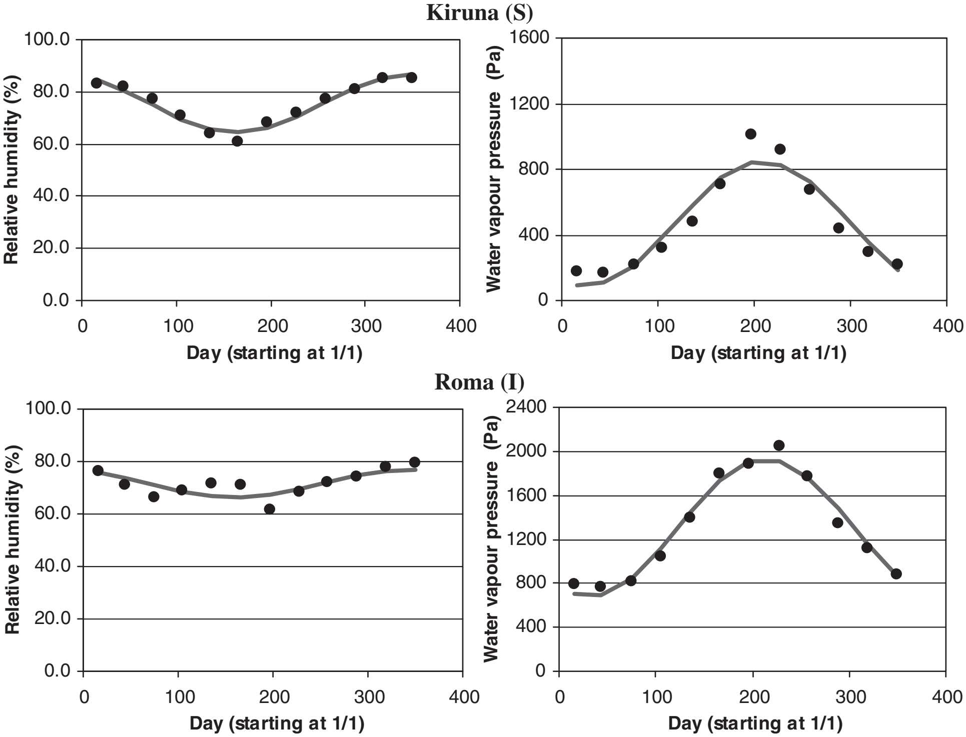

Figure 1.12 Monthly mean relative humidity and vapour pressure in Kiruna (Sweden), a cold climate, and in Rome (Italy), a rather warm climate – harmonic fit.

illustrates, deviation from the monthly averages can be significant:

$$\phi_e = \overline{\phi}_e + \hat{\phi}_e \cos\left[\frac{2\pi(t-d)}{365.25}\right] \quad p_e = \overline{p}_e + \hat{p}_e \cos\left[\frac{2\pi(t-d)}{365.25}\right] \tag{1.24}$$

with:

	Relative humidity (RH), %			Vapour pressure (p), Pa			Quality of the fit
	Average	Amplitude	d Days	Average	Amplitude	d Days	
Kiruna	75.5	11.1	346	469	380	209	$RH\pm$, $p-$
Roma	71.6	5.3	342	1305	627	214	$RH-$, $p\pm$

1.2.5 Wind

Wind impacts the hygrothermal response of building enclosures. A higher speed hastens the initial drying period but lowers the sol-air temperature and counteracts under-cooling. The thermal transmittance of single glass is increased as wind speed increases. Also infiltration, exfiltration and wind washing of poorly mounted insulation layers becomes more importance. Wind combined with precipitation gives wind-driven rain. Wind also governs comfort conditions outdoors. High speeds exert unpleasant dynamic forces on people, chills them and makes it harder to open and close doors.

1.2.5.1 Wind speed

In meteorology, wind speed is seen as a horizontal vector, whose amplitude and direction are measured in the open field at a height of 10 m. The average per 3 seconds is referred to as the immediate, and the average per 10 minutes as the mean speed. The spectrum shows various harmonics, while the vector changes direction constantly. Locally, the environment impacts the amplitude and direction. Venturi effects in small passages increase speed, while alongside buildings eddies develop and the windward and leeward side see zones of still air created.

As following formula shows, due to the friction that terrain roughness causes, wind speed increases from 0 m/s at grade up to a fixed value in the 500–2000 m thick atmospheric boundary layer in contact with the earth:

$$v_h = v_{10}\, K \ln(h/n) \tag{1.25}$$

v_{10} being the average wind speed in flat open terrain, 10 metres above grade, v_h average wind speed h metres above grade, n terrain roughness and K a friction-related factor:

Terrain upwind	K	n
Open sea	0.128	0.0002
Coastal plain	0.166	0.005
Flat grassland, runway area at airports	0.190	0.03
Farmland with low crops	0.209	0.10
Farmland with tall crops, vineyards	0.225	0.25
Open landscape with larger obstacles, forests	0.237	0.50
Old forests, homogeneous villages and cities	0.251	1.00
City centres with high-rises, industrial developments	≥0.265	≥2

Figure 1.13 and Table 1.7 show the annual distribution of the wind vector over all directions at Uccle. For almost half the year the wind comes from the west through south-west to south. Of course, these distributions differ between locations.

1.2.5.2 Wind pressure

The fact that wind exerts a pressure against any obstacle follows from Bernoulli's law. Without friction the sum of kinetic and potential energy in a moving fluid must remain constant. In a horizontal flow, potential energy is linked to pressure. When an obstacle stops the flow, all kinetic becomes potential, which gives the following as pressure (p_w in Pa):

$$p_\mathrm{w} = \rho_\mathrm{a} v_\mathrm{w}^2/2 \tag{1.26}$$

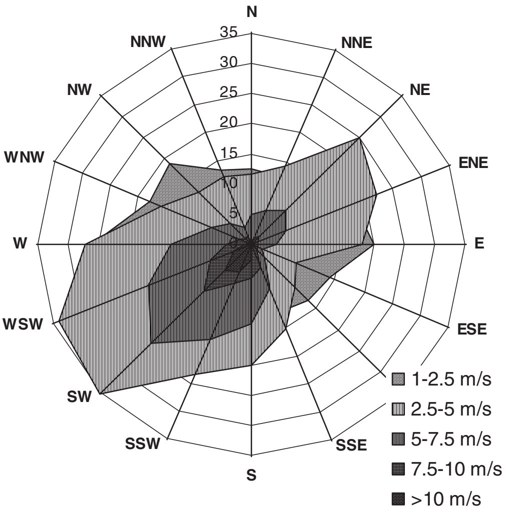

Figure 1.13 Typical wind rose for Uccle, Belgium.

Table 1.7 Uccle, ‰ of the time wind comes from the different directions (monthly means, 1931–1960).

Orientation	Month											
	J	F	M	A	M	J	J	A	S	O	N	D
N	18	22	43	54	59	65	57	37	54	22	15	14
NNE	20	32	48	59	62	60	57	38	47	33	30	13
NE	41	65	79	103	85	72	64	44	67	65	58	47
ENE	54	65	68	68	75	56	40	38	62	63	56	56
E	56	61	48	53	72	45	34	41	63	63	64	41
ESE	28	32	30	28	39	25	26	25	34	38	32	29
SE	36	38	34	33	31	25	25	28	45	50	39	35
SSE	60	53	57	40	38	29	26	36	55	70	60	65
S	90	98	81	49	52	44	44	53	62	100	92	109
SSW	120	109	86	62	70	55	64	88	71	118	105	132
SW	163	130	113	105	92	103	131	152	104	124	142	147
WSW	125	115	100	97	92	100	120	145	103	85	119	125
W	92	73	79	78	71	95	109	121	94	77	89	91
WNW	50	49	54	59	49	74	68	64	55	46	51	46
NW	28	35	73	62	59	84	76	50	44	26	29	32
NNW	19	23	37	50	54	68	59	40	40	20	19	18

Table 1.8 Wind pressure coefficients. Exposed building, up to three storeys, rectangular floor plan, length-to-width ratio 2 to 1 (reference speed: local, at building height).

Location		Wind angle							
		0	45	90	135	180	225	270	315
Face 1	(Wind side)	0.5	0.25	−0.5	−0.8	−0.7	−0.8	−0.5	0.25
Face 2	(Rear side)	−0.7	−0.8	−0.5	0.25	0.5	0.25	−0.5	−0.8
Face 3	(Side wall)	−0.9	0.2	0.6	0.2	−0.9	−0.6	−0.35	−0.6
Face 4	(Side wall)	−0.9	−0.6	−0.35	−0.6	−0.9	0.2	0.6	0.2
Roof Pitches	Wind side	−0.7	−0.7	−0.8	−0.7	−0.7	−0.7	−0.8	−0.7
<10°	Rear side	−0.7	−0.7	−0.8	−0.7	−0.7	−0.7	−0.8	−0.7
Average		−0.7	−0.7	−0.8	−0.7	−0.7	−0.7	−0.8	−0.7
Pitches	Wind side	−0.7	−0.7	−0.7	−0.6	−0.5	−0.6	−0.7	−0.7
10–30°	Rear side	−0.5	−0.6	−0.7	−0.7	−0.7	−0.7	−0.7	−0.6
Average		−0.6	−0.65	−0.7	−0.65	−0.6	−0.65	−0.7	−0.65
Pitches	Wind side	0.25	0	−0.6	−0.9	−0.8	−0.9	−0.6	0
>30°	Rear side	−0.8	−0.9	−0.6	0	0.25	0	−0.6	−0.9
Average		−0.28	−0.45	−0.6	−0.45	−0.28	−0.45	−0.6	−0.45

with ρ_a the air density in kg/m^3 ($\approx$1.2 kg/m^3) and v_w the wind speed in m/s. Yet, since no obstacle stretches to infinity, the flow is only impeded and redirected. That makes wind pressure on buildings different from the stop-the-flow value, a fact accounted for by the pressure coefficient (C_p):

$$p_w = \rho_a C_p v_w^2/2 \tag{1.27}$$

where v_w is a reference wind speed measured at the nearest weather station or at 1 m above the roof ridge. Field measurements, wind tunnel experiments and CFD have shown that pressure coefficients change depending on the reference and the up- and downwind environment. On buildings, their value varies from place to place, being highest at the edges and upper corners, lowest down in the middle. At the wind side, values are positive, at the rear side and sides parallel or nearly parallel to the wind negative. Values are found in the literature, see Table 1.8.

1.2.6 Precipitation and wind-driven rain

In humid climates, rain is the largest moisture load on buildings. The term ‘wind-driven’ applies to the horizontal component, and ‘precipitation’ to the vertical one. While in windless weather the horizontal component remains zero, higher wind speeds increase it. Horizontal and angled outside surfaces collect rain under all circumstances whereas

Table 1.9 Precipitation: duration and amounts per month, means for Uccle (1961–1970).

Precipitation	Month											
	J	F	M	A	M	J	J	A	S	O	N	D
Duration (h)	53.6	57.3	51.9	51.5	41.9	36.0	42.9	38.8	36.5	52.5	67.3	72.7
Amount (l/m^2)	57.4	61.4	56.8	63.6	63.1	74.9	92.3	78.6	54.6	74.5	76.5	84.5

vertical surfaces are struck by wind-driven rain only, albeit that they also suffer from run-off coming from angled and sometimes horizontal surfaces. In countries where outside wall buffering ensures rain-tightness, wind-driven rain to some extent impacts end energy use for heating and cooling.

1.2.6.1 Precipitation

Precipitation is as variable as the wind. Table 1.9 and Figure 1.14 give mean durations (hours) and amounts per month for Uccle. As with wind speed, no annual cycle appears, though slightly more rain falls in summer. The absolute maxima noted between 1956 and 1970 were: 4 l/m^2 in 1 minute, 15 l/m^2 in 10 minutes and 42.8 l/m^2 in 1 hour.

Showers are characterized by a droplet distribution $F_{\text{d,precip}}$. According to Best (1950), the relation with rain intensity is:

$$F_{\text{d,precip}} = 1 - \exp\left[-\left(\frac{d}{1.3 g_{\text{r,h}}^{0.232}}\right)^{2.25}\right] \tag{1.28}$$

with d the droplet size in m and $g_{\text{r,h}}$ the precipitation in l/(m^2.h). In windless weather, droplets have a final speed (d droplet size in mm, see also Figure 1.15) given by:

$$v_\infty = -0.166033 + 4.91844d - 0.888016d^2 + 0.054888d^3 \tag{1.29}$$

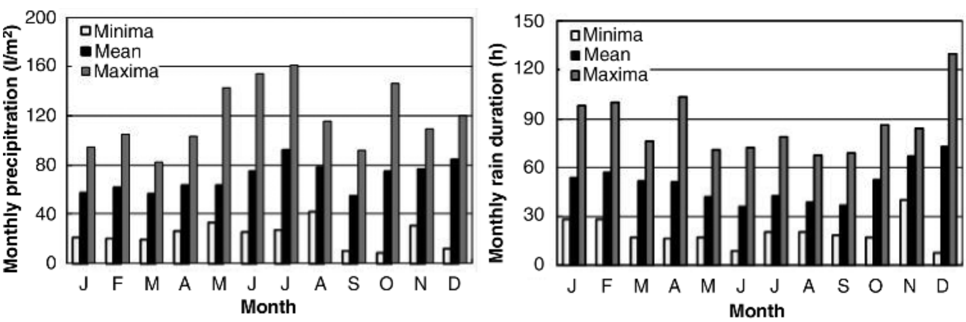

Figure 1.14 Precipitation: monthly amounts and duration for 1961–1970 at Uccle (averages, maxima and minima).

Depending on the mean droplet size, following terms describe precipitation:

Mean droplet size, mm	Precipitation
0.25	Drizzle
0.50	Normal
0.75	Strong
1.00	Heavy
1.50	Downpour

1.2.6.2 Wind-driven rain

The drag force that wind exerts inclines droplet trajectories. Final tilt angle depends on droplet size, wind direction compared to horizontal and speed increase with height. A constant horizontal speed keeps the inclined droplet trajectories straight. Wind-driven rain intensity ($g_{\mathrm{r,v}}$ in kg/(m^2.s)) then becomes:

$$g_{\mathrm{r,v}} = 0.222 v_{\mathrm{w}} g_{\mathrm{r,h}}^{0.88} \tag{1.30}$$

with $g_{\mathrm{r,h}}$ the precipitation in kg/(m^2.s). This equation is simplified to:

$$g_{\mathrm{r,v}} = 0.2 v_{\mathrm{w}} g_{\mathrm{r,h}} \tag{1.31}$$

a relation that fits well in open field. For wind speeds beyond 5 m/s, wind-driven rain exceeds precipitation there. In built environments, the equation fails. Intensity on a facade in fact depends on horizontal rain intensity, raindrop size distribution, building volumes up and down wind, building geometry, building orientation compared to wind direction, where on the enclosure and local detailing. Buildings in an open neighbourhood may catch 40 times as much wind-driven rain as buildings in a densely built environment. Local amounts on the facade are linked to the wind flow pattern around the building. For low-rises, the upper corners see the highest values. Under drizzle,

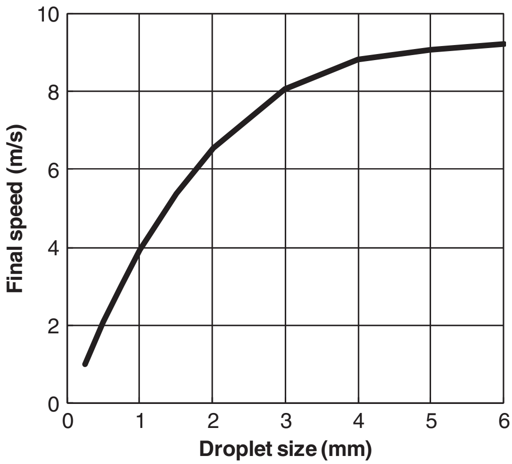

Figure 1.15 Final vertical speed of a raindrop in windless weather.

Table 1.10 Wind-driven rain on an 18-storey block of flats in Munich, measured by the Fraunhofer Institut für Bauphysik, May–November 1972.

Spot	Wind-driven rain, kg/m^2
Facade west, middle 3th floor	29
Facade west, middle 9th floor	55
Facade west, middle 16th floor	65
Roof edge north	115
Roof edge south	130

high-rises catch most at the highest floors, the higher edges and the upper corners. The differences diminish with higher rain intensity and wind speed. Measured deposits on an 18-storey block of flats, listed in Table 1.10, underline these trends.

The formula used to describe local wind-driven rain intensity on building enclosures is:

$$g_{r,v} = (0.2 C_r v_w \cos\theta) g_{r,h} \tag{1.32}$$

with θ the angle between wind direction and normal to the surface and C_r the wind-driven rain factor, a function of the type of precipitation, the surroundings, the facade spot in question, local detailing, and so on. On average, C_r is between 0.25 and 2. The product $0.2C_r v_w \cos\theta$ is called the 'catch ratio', the amount of wind-driven rain hitting a facade spot as a fraction of the precipitation in the open field during the same rain event. The formula is based on experimental evidence. For that, catch ratios on the south-west facade of a test building, calculated using CFD for the wind field and droplet tracing for the rain trajectories, were compared with measured data, see Figure 1.16. Both fit reasonably well.

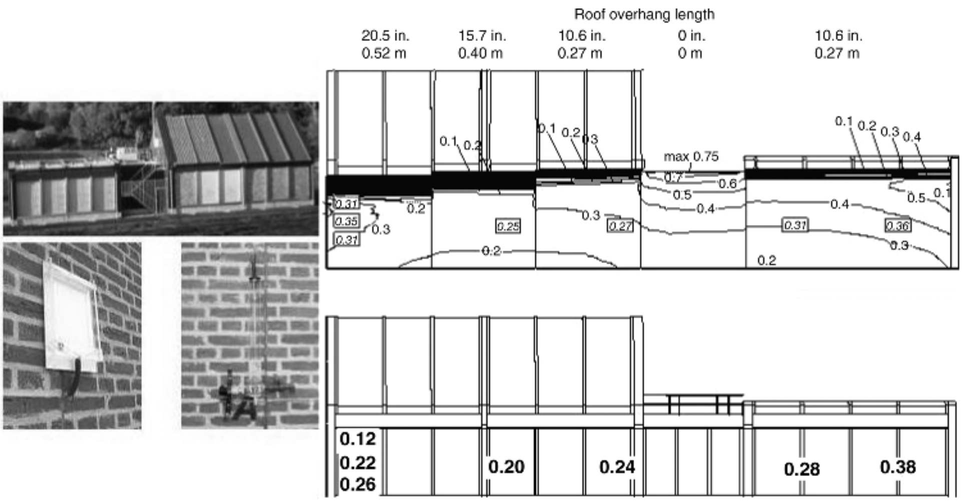

Figure 1.16 SW facade of a test building: calculated lines (top) of equal catch ratio using CFD and droplet tracing compared to measured catches (below).

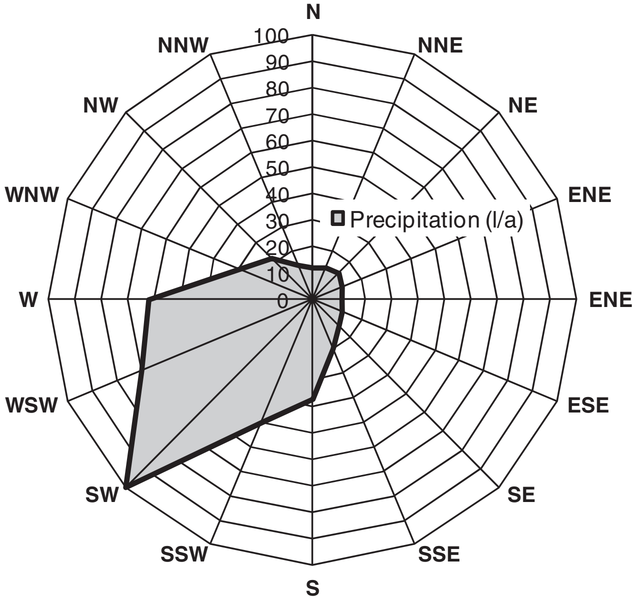

Figure 1.17 Average rain rose for Uccle.

In north-western Europe and as Figure 1.17 confirms for Uccle, wind-driven rain mainly comes from the south-west. Happily, strong winds and heavy precipitation rarely coincide. Between 1956 and 1970 the largest hourly means measured at Uccle were:

Precipitation, l/h	Mean wind speed, m/s
15	5.8
42	2.2

1.2.7 Microclimates around buildings

The microclimate around buildings is a complex reality. The immediate environment has an important impact, as it affects shading, wind direction and speed, wind-driven rain patterns, temperatures and so on. But also each part of the enclosure experiences differences, depending on factors such as slope and orientation, its position, whether or not it is shaded and/or sheltered by protrusions and volumes above. All these have impacts on the damage tolerance of a building.

This complexity, including the ever-changing, time-dependent character of the weather, forces us to simplify, using design temperatures, reference days, reference years, indoor climate classes, and so on. It must therefore be admitted that any evaluation using these, results in an approximate picture of reality, loaded with uncertainty.

1.2.8 Standardized outdoor climate data

1.2.8.1 Design temperature

In north-west European countries with massive building tradition, the design temperature (θ_{ed}, °C) for heating is either the lowest running two-day mean over a period of 20 or the lowest daily mean over a period of 10 years. Many countries have maps giving values. In the USA and Canada, two countries with a timber-frame tradition, heating designers can choose between two hourly values: one exceeded 99.6% or 99% of the time during $8790 \times T$ hours with T the years considered, actually 1986–2010. For cooling, the hourly mean exceeded 0.4% or 1% of the time is used. The same holds for the wet bulb temperatures, needed to calculate the power that (de)humidification requires.

Both approaches remain quite close. Take for example Uccle. The two-day mean for the period 1971–1990 is −8 °C. The 99.6% and 99% hourly means for the period 1986–2010 are −6.6 °C and −4.4 °C, respectively. The fact that the period used by the USA and Canada misses the cold winter of 1979 explains most of the difference.

1.2.8.2 Reference years

Air temperature, solar radiation, longwave radiation and wind are of decisive importance for the net heating and cooling demand and overheating risk. To allow the use of building energy simulation tools (BES), hourly thermal reference years (TRYs) were constructed. Mean ones give the same annual net heating and cooling demand as found on average over, for example, 30 successive years. Warm ones help in evaluating overheating and allow a better guess of the cooling load. Cold ones do the same for the heating load. TRYs exist for several locations worldwide. For steady state calculations, monthly TRYs are used. The Belgian three used the 1931–1960 averages and standard deviations. For the mean, cold and warm year, see Table 1.11. Cloudiness J in the table stands for the ratio between the actual and clear sky solar radiation on a horizontal surface. The energy performance of buildings TRY in that country however took the 1961–1990 averages with temperature, total ($E_{ST,hor}$) and diffuse solar radiation ($E_{sd,hor}$) on a horizontal surface as parameters, see Table 1.12.

1.2.8.3 Very hot summer, very cold winter day

A simpler choice than using TRYs is looking for a hot summer's day and a cold winter's day with probability once in, for example, 20 years, and considering both as being the last of a spell of the same hot and cold days. This allows analytic solutions to be used for the transient response. Table 1.13 lists the two for Uccle. They are slightly reframed to fit the spell assumption.

1.2.8.4 Moisture reference years

Since the end of the 1960s, calculation tools have allowed us to predict the moisture response of assemblies. They require, among others, knowledge of the indoor and outdoor ambient conditions. So, the 1990s saw the introduction of the concept of moisture reference year, the year with return rate one in every ten years giving the

Table 1.11 Monthly mean TRYs for Belgium (mean, *cold*, **warm**).

Month	θ_e (°C)	$E_{ST,hor}$(W/m^2)	Wind (m/s)	*RH* (%)	*p* (Pa)	*J* (−)
January	3.8	26.6	3.8	91	730	0.52
February	3.2	55.2	5.1	87	668	0.58
March	7.1	88.5	3.9	85	857	0.56
April	9.1	131.4	4.7	81	935	0.56
May	11.9	172.6	3.4	77	1072	0.59
June	16.7	216.9	3.2	80	1520	0.68
July	16.1	162.5	3.0	79	1445	0.53
August	17.1	158.0	3.5	83	1618	0.60
September	14.3	128.7	3.4	83	1352	0.67
October	11.0	64.9	3.6	91	1194	0.54
November	6.1	29.6	3.8	91	856	0.45
December	3.1	19.3	3.6	91	694	0.46
January	*−3.9*	*33.2*	*4.1*	*86*	*379*	*0.65*
February	*−1.4*	*63.1*	*3.3*	*85*	*462*	*0.66*
March	*3.1*	*94.3*	*3.6*	*81*	*618*	*0.59*
April	*6.7*	*101.5*	*4.0*	*87*	*853*	*0.43*
May	*10.8*	*151.5*	*3.7*	*84*	*1087*	*0.51*
June	*14.2*	*178.7*	*3.1*	*79*	*1278*	*0.56*
July	*16.1*	*171.4*	*3.7*	*80*	*1463*	*0.55*
August	*15.9*	*136.7*	*3.5*	*86*	*1552*	*0.52*
September	*12.8*	*123.0*	*2.9*	*82*	*1211*	*0.64*
October	*7.5*	*53.9*	*3.3*	*90*	*932*	*0.44*
November	*4.2*	*40.2*	*4.6*	*88*	*725*	*0.62*
December	*0.2*	*25.3*	*3.2*	*90*	*558*	*0.61*
January	**6.8**	**25.3**	**5.2**	**87**	**859**	**0.50**
February	**7.6**	**55.4**	**4.4**	**89**	**928**	**0.58**
March	**8.5**	**109.4**	**3.5**	**85**	**942**	**0.69**
April	**12.3**	**130.7**	**3.0**	**86**	**1229**	**0.55**
May	**15.4**	**206.8**	**2.8**	**72**	**1258**	**0.70**
June	**18.8**	**235.2**	**3.1**	**74**	**1605**	**0.74**
July	**20.0**	**242.9**	**3.5**	**73**	**1706**	**0.79**
August	**19.9**	**181.7**	**2.9**	**74**	**1718**	**0.69**
September	**16.5**	**171.0**	**3.5**	**70**	**1313**	**0.89**
October	**13.8**	**86.2**	**2.6**	**86**	**1356**	**0.71**
November	**9.4**	**35.1**	**5.1**	**88**	**1036**	**0.54**
December	**7.4**	**15.4**	**5.3**	**87**	**895**	**0.37**

Table 1.12 Energy performance legislation, reference year for Belgium.

Month	θ_e (°C)	$E_{ST,hor}$ (MJ/m^2)	$E_{sd,hor}$ (MJ/m^2)
January	3.2	71.4	51.3
February	3.9	127.0	82.7
March	5.9	245.5	155.1
April	9.2	371.5	219.2
May	13.3	510.0	293.5
June	16.3	532.4	298.1
July	17.6	517.8	305.8
August	17.6	456.4	266.7
September	15.2	326.2	183.6
October	11.2	194.2	118.3
November	6.3	89.6	60.5
December	3.5	54.7	40.2

highest wetness in an assembly. Each moisture event, however, demanded another year. A wet and windy one best serves for rain leakage. Solar-driven vapour flow scores highest in years with sunny summers, interrupted by regular rainy spells. Interstitial condensation is worst in cold, humid ones with little sun in summer. Initially, the exercise ran for interstitial condensation only, see Table 1.14.

An alternative consists of using a so-called moisture index. As more wetting and less drying decreases moisture tolerance, this index must combine the two. In Canada, the exercise bases on normalized wetting (WI_{norm}) and drying (DI_{norm}) functions:

$$WI_{norm} = \frac{WI - WI_{min}}{WI_{max} - WI_{min}} \qquad DI_{norm} = \frac{DI - DI_{min}}{DI_{max} - DI_{min}} \tag{1.33}$$

where WI equals the annual amount of wind-driven rain hitting a facade with given orientation at the location considered and DI is:

$$DI = \sum_{h=1}^{k} \overline{x}_{sat}\left(1 - \overline{\phi}\right)$$

with $\overline{x}_{sat}$ the hourly mean vapour saturation ratio, $\overline{\phi}$ the hourly mean relative humidity outdoors at that location and Σ denoting the sum of all hourly means over a year. The minimums WI_{min} and DI_{min} and maximums WI_{max} and DI_{max} represent the most and least severe year in Ottawa out of a file of 30. For any other location, WI and DI are taken from the third year in terms of severity over the 30 years of hourly data there. The moisture index then is:

$$MI = \sqrt{WI_{norm}^2 - (1 - DI_{norm})^2} \tag{1.34}$$

Table 1.13 Uccle: cold winter (declination −17.7°) and hot summer day (declination 17.7°).

Hour↓	Cold winter day			Hot summer day		
	Temp. °C	Direct sun, ⊥, W/m^2	Diffuse sun, horizontal, W/m^2	Temp. °C	Direct sun, ⊥, W/m^2	Diffuse sun, horizontal, W/m^2
0	−13.3	0	0	20.2	0	0
1	−13.6	0	0	19.8	0	0
2	−13.8	0	0	19.5	0	0
3	−14.2	0	0	19.0	0	0
4	−14.6	0	0	18.5	0	0
5	−15.0	0	0	18.0	136	6
6	−15.4	0	0	17.8	301	50
7	−15.5	0	0	17.8	440	87
8	−15.5	42	8	20.0	555	121
9	−14.9	336	47	22.0	645	146
10	−14.3	553	72	25.5	711	165
11	−13.1	636	89	28.0	752	180
12	−11.8	669	100	30.0	768	187
13	−11.7	656	105	30.8	759	188
14	−11.5	611	94	30.5	726	179
15	−11.9	564	72	30.0	669	165
16	−12.3	375	39	29.0	587	147
17	−12.8	47	11	27.8	480	121
18	−13.3	0	0	26.5	348	90
19	−13.7	0	0	25.5	192	49
20	−14.0	0	0	24.2	11	7
21	−14.5	0	0	23.0	0	0
22	−15.0	0	0	22.0	0	0
23	−15.1	0	0	20.5	0	0
24	−15.2	0	0	20.2	0	0

This index has two drawbacks. First it only considers problems caused by wind-driven rain, overlooking problematic moisture deposits due to interstitial condensation. Secondly, it excludes the effects of solar radiation, although drying primarily depends on the difference between the vapour saturation ratio at the surface and the vapour ratio in the air, a reality that the sun heavily impacts.

1.2.8.5 Equivalent temperature for condensation and drying

In cold and temperate climates interfaces where interstitial condensate deposits sit at the outside of the thermal insulation, where the remaining thermal resistance to outdoors is

Table 1.14 Moisture reference years for interstitial condensation, four European cities.

Month	Uccle			Rome			Copenhagen			Luleå		
	θ_e °C	p_e Pa	$E_{ST,h}$ W/m^2	θ_e °C	p_e Pa	$E_{ST,h}$ W/m^2	θ_e °C	p_e Pa	$E_{ST,h}$ W/m^2	θ_e °C	p_e Pa	$E_{ST,h}$ W/m^2
J	2.7	675	24.0	8.0	747	73.3	−0.1	569	18.2	−12.6	190	2.4
F	1.7	587	50.4	10.1	877	205.3	−0.4	507	53.1	−13.2	183	22.9
M	5.9	724	99.0	10.2	811	257.8	−0.3	476	83.4	−5.2	357	54.8
A	8.5	932	115.5	13.2	997	289.2	7.4	817	159.6	−2.4	415	109.8
M	12.6	1123	180.0	18.3	1323	243.6	12.0	1080	227.5	3.6	538	179.6
J	15.5	1374	215.0	22.3	1733	257.0	14.7	1355	229.4	10.8	894	234.4
J	14.9	1423	148.2	24.5	1976	271.1	15.3	1474	186.3	15.4	1365	203.9
A	16.2	1492	172.8	22.3	1747	224.0	15.1	1435	178.3	12.3	1144	122.6
S	13.5	1300	120.6	19.4	1524	187.8	12.6	1275	125.4	7.7	883	71.2
O	11.1	1097	102.1	17.1	1446	125.5	7.7	961	54.9	−2.4	430	28.4
N	4.0	716	40.1	11.5	1029	74.9	5.0	793	26.6	−4.1	401	4.3
D	4.8	783	15.6	9.6	907	51.2	1.1	614	15.9	−17.1	123	0.5

mostly small. In these interfaces, vapour saturation pressure fluctuates with temperature. As the relation between the two is exponential, higher interface temperatures have a greater weight on the mean vapour saturation pressure. So, over a month, that mean will differ from the value at the mean interface temperature. It is therefore sensible to calculate it beforehand and link its value to a 'fictive' outdoor temperature, called the 'equivalent temperature for condensation and drying', which works due to the low remaining thermal resistance to outdoors.

Quantification goes as follows. First, the sol-air temperature per orientation and slope is calculated for each month, using hourly temperature, solar and longwave radiation data. Then, the hourly temperatures in the condensation interface are fixed. As it sits close to outdoors, a steady-state approach suffices:

$$\theta_j = \theta_e^* + R_e^j\left(\theta_i - \theta_e^*\right)/R_a \tag{1.35}$$

with θ_i the temperature indoors, θ_e^* the sol-air temperature, R_e^j the thermal resistance from the condensation interface to outdoors and R_a the thermal resistance of the assembly environment to environment. Next, vapour saturation pressure is linked to these hourly interface temperatures and the mean for the month considered is calculated as:

$$\overline{p}_{sat,j} = \frac{1}{T}\int_o^T p_{sat,j}\,dt \tag{1.36}$$

Table 1.15 Uccle, equivalent temperature for condensation and drying ($a_K = 1$, $e_L = 0.9$).

Slope Az.	Annual mean $\overline{\theta}^*_{ce}$ (°C)					Annual amplitude $\hat{\theta}^*_{ce}$ (°C)				
	N	NW/NE	W/E	SW/SE	S	N	NW/NE	W/E	SW/SE	S
0	14.4	14.4	14.4	14.4	14.4	12.6	12.6	12.6	12.6	12.6
15	13.7	13.9	14.4	14.7	14.8	12.4	12.5	12.6	12.7	12.7
30	12.9	13.4	14.2	14.9	16.0	11.7	12.0	12.3	12.4	12.4
45	12.2	12.8	13.9	14.7	14.9	10.9	11.3	11.6	12.0	11.8
60	11.9	12.6	13.7	14.6	14.7	9.8	10.6	11.2	11.3	11.1
75	11.8	12.4	13.5	14.3	14.6	9.3	10.0	10.7	10.6	10.3
90	12.1	12.6	13.6	14.2	14.4	9.1	9.5	9.9	9.7	9.5

Related interface temperature is then:

$$\overline{\theta}^*_{\overline{p}_{sat,j}} = F\left(\overline{p}_{sat,j}\right) \tag{1.37}$$

From it, the monthly mean equivalent temperature for condensation and drying follows:

$$\overline{\theta}^*_{ce} = \frac{\overline{\theta}_{\overline{p}_{sat,j}} + \overline{\theta}_i\left(R_e^j/R_a\right)}{1 - R_e^j/R_a} \approx \frac{\overline{\theta}_{\overline{p}_{sat,j}}}{1 - R_e^j/R_a} \tag{1.38}$$

The almost equal to sign ≈ indicates that the ratio R_e^j/R_a is so small that neglecting its product with the indoor temperature has virtually no impact, a fact that anyhow introduces some uncertainty.

Once this is done for all months, the annual mean is fixed and the first and second harmonic transposed into an annual amplitude, and a time function $C(t)$. Table 1.15 gives the mean and amplitude for a non-shaded, sun-radiated surface with shortwave absorptivity 1 and longwave emissivity 0.9 for Uccle, while Table 1.16 lists the time function.

Correction for non-shaded, sun-radiated surfaces with different shortwave absorptivity first requires combining the annual mean and amplitude into a relation of the form:

$$\theta^*_{ce} = \overline{\theta}^*_{ce} + \hat{\theta}^*_{ce} C(t) \tag{1.39}$$

Table 1.16 Uccle, month-based time function.

Month	$C(t)$	Month	$C(t)$	Month	$C(t)$	Month	$C(t)$
January	−0.98	April	−0.10	July	+1.00	October	−0.10
February	−0.85	May	+0.55	August	+0.85	November	−0.55
March	−0.50	June	+0.90	September	+0.55	December	−0.90

Then the mean and amplitude are adapted to account for the actual shortwave absorptivity:

$$\left[\overline{\theta}^*_{ce}\right] = \alpha_K\left(\overline{\theta}^*_{ce} - \overline{\theta}'_e\right) + \overline{\theta}'_e \quad \left[\hat{\theta}^*_{ce}\right] = \alpha_K\left(\hat{\theta}^*_{ce} - \hat{\theta}'_e\right) + \hat{\theta}'_e \tag{1.40}$$

In these equations $\overline{\theta}'_e$ and $\hat{\theta}'_e$ are the annual mean and amplitude of the equivalent temperature for condensation and drying on a north-facing surface with slope of 45°, shortwave absorptivity 0 and longwave emissivity 0.9, equal to 8.5 and 7.1 °C at Uccle. If the longwave emissivity is also 0 or the surface stays shaded, the mean and amplitude of the air temperature take over, 9.8 and 6.9 °C at Uccle. For non-shaded, sun-radiated surfaces with longwave emissivity between 0 and 0.9, a linear interpolation applies for $\overline{\theta}'_e$ and $\hat{\theta}'_e$:

$$\overline{\theta}'_e = 8.5 + 1.3\left(\frac{0.9 - e_L}{0.9}\right) \quad \hat{\theta}'_e = 7.1 - 0.2\left(\frac{0.9 - e_L}{0.9}\right) \tag{1.41}$$

The effective monthly mean equivalent temperature for condensation and drying on a non-shaded, sun-radiated surface then becomes:

$$\left[\theta^*_{ce}\right] = \left[\overline{\theta}^*_{ce}\right] + \left[\hat{\theta}^*_{ce}\right]C(t) \tag{1.42}$$

An estimate for sun-radiated surfaces that get shade during part of the day consists of adapting Eq. (1.40):

$$\left[\overline{\theta}^*_{ce}\right] = \alpha_K\left(\overline{\theta}^*_{ce} - \overline{\theta}'_e\right)\frac{E_{s,T,real}}{E_{s,T}} + \overline{\theta}'_e \quad \left[\hat{\theta}^*_{ce}\right] = \alpha_K\left(\hat{\theta}^*_{ce} - \hat{\theta}'_e\right)\frac{E_{s,T,real}}{E_{s,T}} + \hat{\theta}'_e \tag{1.43}$$

with $E_{s,T}$ the total monthly solar radiation that the surface should receive, if non-shaded, and $E_{s,T,real}$ the total monthly solar radiation actually recorded.

Calculating the equivalent temperature for condensation and drying for any other cold or temperate climate location proceeds as explained.

1.2.8.6 Monthly mean vapour pressure outdoors

The monthly mean vapour pressure outdoors is quantified using the same time function C(t):

$$p_e = \overline{p}_e + \hat{p}_e C(t) \tag{1.44}$$

with $\overline{p}_e$ the annual mean and $\hat{p}_e$ the amplitude, in Uccle 1042 and 430 Pa.

1.3 Indoors

Building use presumes comfortable temperatures. Whether or not relative humidity demands control depends on climate and building use. Those two and the air pressure differences between rooms and outdoors fix the environmental load that the enclosure has to endure.

1.3.1 Air temperatures

1.3.1.1 In general

The air temperature not only affects thermal comfort but also impacts the end energy use for heating and cooling plus the enclosure's moisture response. Standards focus

Table 1.17 Operative temperatures needed according to DIN 4701 and EN 12 831.

Building type	Room	Temperature	
		DIN 4701	EN 12831
Dwelling	Daytime room and bedroom	20	20
	Bathroom	24	24
Hospital	Nursery	22	20
	Surgery, premature births	25	
Office buildings	All rooms	20	20
	Corridors, rest rooms	15	
Indoor swimming pool	Natatorium	28	
	Showers	24	
	Cabins	22	
Schools	Classroom		20
Department store			20
Church			15
Museum, gallery			16

on the operative temperature, see Table 1.17, but in most buildings, air temperature is the factor that is controlled, although a thermostat somewhere on a wall senses a mixture of the local air and surface temperatures, the two impacted by the little heat that the device produces. In insulated buildings, operative and air temperature hardly differ.

1.3.1.2 Measured data

Residential buildings – Figure 1.18 shows weekly mean air temperatures measured between 1972 and 2008 in 283 daytime rooms, 338 bedrooms and 37 bathrooms of poorly insulated homes. The figures picture the data as a function of the mean outdoor temperature for the same week. Between 2002 and 2005, data was also collected in 39 well-insulated homes. Table 1.18 lists the regression line constants and correlation coefficient for the two sets.

In the poorly insulated dwellings, the weekly daytime room means are near to the comfort value with only a limited impact of the mean outdoors, proving these rooms are on average well heated. Bedrooms and bathrooms instead show significantly lower

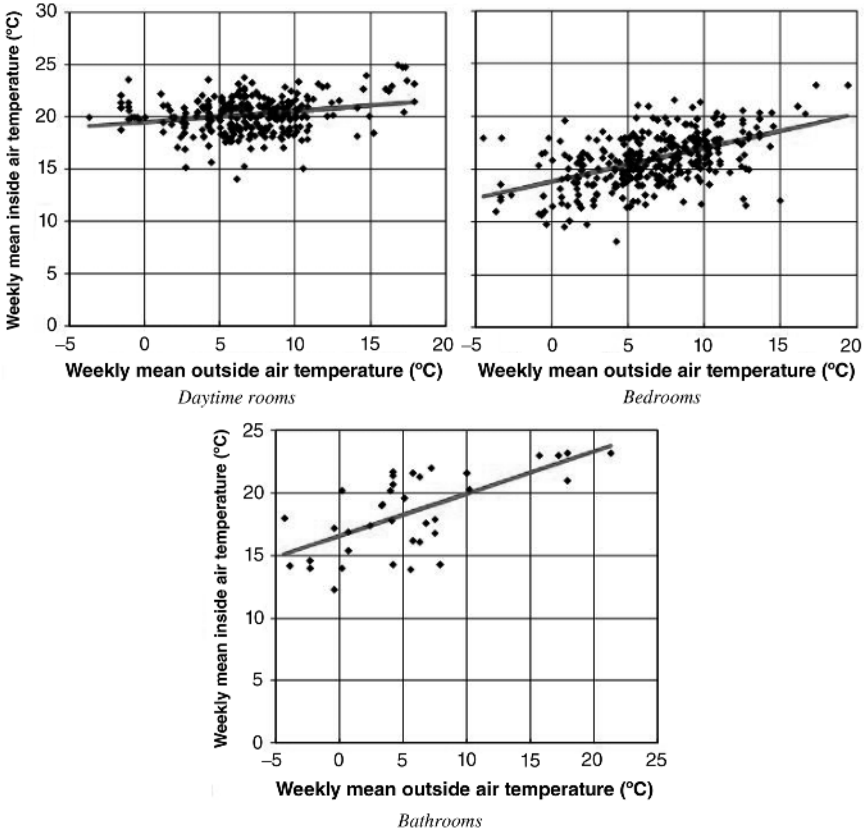

Figure 1.18 Poorly insulated dwellings: weekly mean inside air temperatures in a daytime rooms (top left), bedrooms (top right) and bathrooms (below).

Table 1.18 Measured weekly mean air temperatures.

	Number of weekly records	$\overline{\theta}_i = a + b\overline{\theta}_e$		Correlation coefficient
		a (°C)	b (–)	
Poorly insulated homes				
Daytime rooms	283	19.5	0.11	0.06
Bedrooms	338	13.8	0.32	0.26
Bathrooms	37	16.5	0.34	0.43
Insulated homes				
Daytime rooms	39	19.3	0.22	0.89
Bedrooms	78	15.6	0.42	0.95
Bathrooms	39	19.9	0.20	0.82

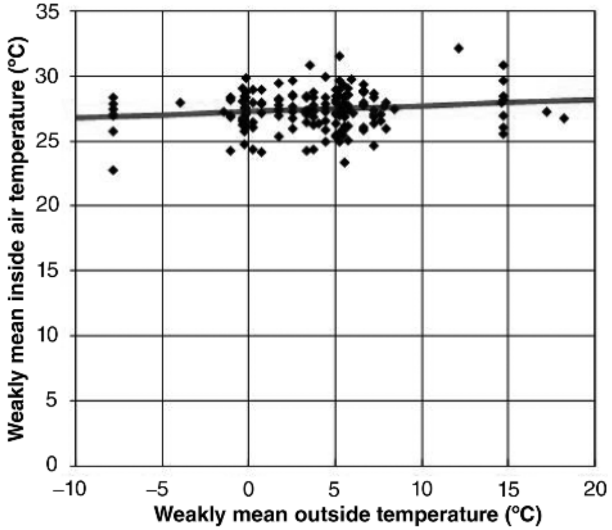

Figure 1.19 Natatoriums: weekly mean inside temperature.

weekly means that change strongly with the mean outdoors. While bathrooms look intermittently heated, bedrooms apparently lack heating. Their indoor temperature merely reflects the balance between transmission and ventilation gains from adjacent rooms, transmission and ventilation losses to outdoors, solar gains through the window and internal gains. Insulated, the conclusions differ. Daytime rooms remain well heated but bedrooms look warmer, probably due to the better insulation, although still, they are either intermittently or poorly heated. Bathrooms are also warmer but the outdoor temperature still intervenes.

Poorly heating the sleeping rooms seems a widespread dweller's habit, which has its advantages. For people, facing temperature differences favours health. After all, the blankets ensure comfort while sleeping.

Natatoriums – Figure 1.19 groups 162 weekly mean air temperatures logged in 16 natatoriums, together with the corresponding weekly mean outdoors. The least square line and correlation coefficient are given in Table 1.19.

Table 1.19 Natatoriums, measured weekly mean air temperatures.

	$\theta_i = a + b\theta_e$		
Number of weekly records	a (°C)	b (–)	Correlation coefficient
162	27.3	0.045	0.02

On average, the value measured fits well with the preferred 28 °C operative temperature. Nonetheless, the lowest (22.2 °C) and highest value (32.2 °C) deviate substantially. Well known is that leisure swimmers like higher temperatures, and competition swimmers prefer lower temperatures.

1.3.2 Relative humidity and vapour pressure

Relative humidity and vapour pressure are key factors impacting moisture tolerance. Both also influence the indoor environmental quality. In temperate climates the two are mostly allowed to vary freely. Values depend on the whole building heat, air, moisture balance. Only museums, archives, cleanroom spaces, computer rooms, surgical units and intensive care units require control, as do dwellings in hot and humid or really cold climates.

1.3.2.1 Vapour release indoors

Tables 1.20–1.23 list literature data about the overall daily vapour release, the vapour release per activity and a more detailed overview of the hourly releases by families as function of their living patterns.

Table 1.24 suggests the following relation between vapour release and number of children:

$$G_{\mathrm{v,P}} = 3.2 + 2.8 n_{\mathrm{children}} \quad r^2 = 0.28(\mathrm{kg}/(\mathrm{day.child}))$$

This 2.8 kg looks high. A more modest value is 1 kg extra per day per child listed in the final column of the table.

Table 1.20 Daily vapour release, depending on the number of family members.

Family members	Average water vapour release in kg/day		
	Low water usage[a)]	Average water usage[b)]	High water usage[c)]
1	3 to 4	6	9
2	4	6	11
3	4	9	12
4	5	10	14
5	6	11	15
6	7	12	16

a) Dwelling frequently unoccupied.
b) Families with children.
c) Teenage children, frequent showers, etc.

Table 1.21 Vapour release linked to metabolism, activity and others.

	Activity	Release, g/h
Adults, metabolism	Sleeping	30
	At rest (depends on temperature)	33–70
	Light physical activity	50–120
	Moderate physical activity	120–200
	Heavy physical activity	200–470
Bathroom	Bath (15′)	60–700
	Shower (15′)	≤660
Kitchen	Breakfast preparation (four people)	160–270
	Lunch preparation (four people)	250–320
	Dinner preparation (four people)	550–720
	Dish cleaning by hand	480
	Daily average release	100
Laundry drying	After dry spinning	50–500
	Starting from wet	100–1500
Plants (per pot)		5–20
Young trees		2000–4000
Full-grown trees		$2–4 \times 10^6$

Table 1.22 Vapour release by a family of two.

Hour	Persons present	Release in g/h				Total
		Persons	Cooking	Hygiene	Laundry	
Both working, weekday						
1–5	2	120				120
6	2	120	240	720		1080
7	2	120	240			360
8–17	0					0
18	2	120				120
19–20	2	120	480			600
21–24	2	120				120
Total		1680	1440	1200		4320

Table 1.23 Vapour release by a family of four.

Hour	Persons present	Release in g/h				Total
		Persons	Cooking	Hygiene	Laundry	
Father working, oldest child at school, mother and one child at home, weekday						
1–5	4	240				240
6–7	4	240	480	720		1440
8	2	120			120	240
9	1	120			180	300
10	1	120	720		180	1020
11–12	2	120	1200	120		1440
13–14	2	120	480	120		720
15	2	120			120	240
16–17	2	180			120	300
18	4	240				240
19	4	240	480			720
20	4	240	480	240		960
21–22	4	240				240
23	4	240		240		480
24	4	240				240
Total	4680	6000	2400	840	13 920	

Table 1.24 Daily vapour release in relation to the number of family members (several sources).

Number of family members			
2 (no children)	3 (one child)	4 (two children)	>4 (more children)
8	12	14	>14 +1 kg/(day.child)
	10		
7	20		
		14.6	
13.2	19.9	23.1	
	11.5		
	5–12		
	6–10.5		
4.3		13.7	
8.2	12.1	14.1	14.4
Mean: 8.14	Mean: 11.9	Mean: 15.9	

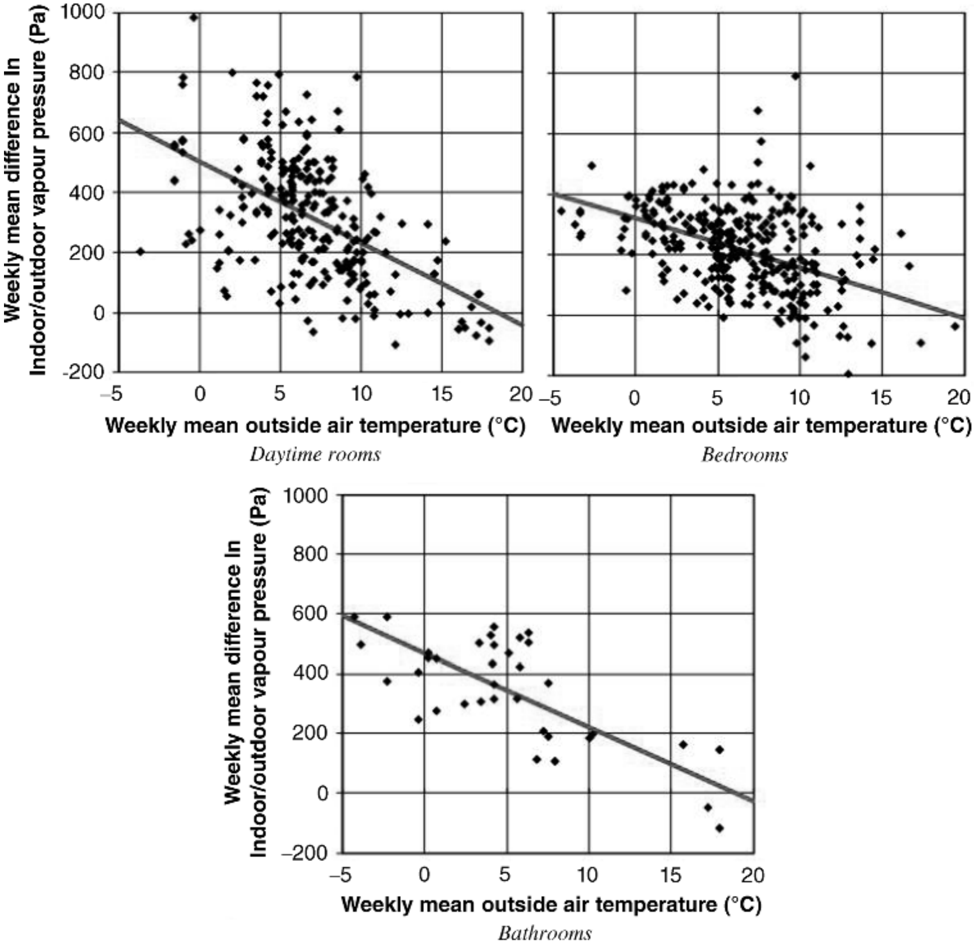

Figure 1.20 Poorly insulated homes: difference in weekly mean inside/outside vapour pressure in daytime rooms (top left), bedrooms (top right) and bathrooms (below).

1.3.2.2 Measured data

Residential buildings – Figure 1.20 displays the weekly mean differences in indoor/outdoor vapour pressure measured between 1972 and 2008 in the 261 daytime room, 315 bedrooms and 37 bathrooms of a number of poorly insulated homes. The figures present the data as a function of the mean air temperature outdoors for the same week. Between 2002 and 2005, data also came from 39 well-insulated homes.

Table 1.25 lists the least square lines, the 95% line and the correlation coefficients. For the poorly insulated dwellings, also a multiple regression between relative humidity and the air temperature indoors and outdoors is included. In general, the difference decreases when it is warmer outdoors. Reasons are more intense ventilation in summer and the

Table 1.25 Measured weekly indoor/outdoor vapour pressure difference and relative humidity.

	Number of records	$\Delta p_{ie} = a + b\theta_e$		Correlation r^2	$\varphi_i = a + b\theta_i + c\theta_e$			Correlation r^2
		a, Pa	b, Pa/°C		a, %	b,%/°C	c, %/°C	
Poorly insulated homes								
Daytime rooms	261	504	−27.2	0.28	99.6	−2.6	−0.87	0.40
95% line		704	−27.2					
Bedrooms	351	319	−16.3	0.19	94.5	−3.4	−1.9	0.47
95% line		465	−16.3					
Bathrooms	37	469	−24.9	0.61	94.5	−2.5	−1.2	0.58
95% line		575	−24.9					
Insulated homes								
Daytime rooms	39	299	−12.4	0.53				
95% line		594	−18.0					
Bedrooms	39	261	−10.7	0.18				
95% line		497	−13.1					
Bathrooms	39	338	−11.3	0.64				
95% line		658	−16.1					

long-term hygric inertia of fabric, furniture and furnishings that dampens and shifts the annual amplitude indoors compared to outdoors.

Most humid are the daytime rooms. Relative humidity in all rooms decreases with higher indoor and increases with higher outdoor temperatures. A comparison with the insulated dwellings shows that bedrooms and bathrooms remain quite close but that daytime rooms look much dryer when insulated. Why this should be is unclear. Probably kitchen stove hoods have become standard, or these more recent dwellings have fewer inhabitants, more volume per inhabitant and are better ventilated.

Natatoriums – Figure 1.21 shows 162 records of weekly mean differences in indoor/outdoor vapour pressure in the 16 natatoriums mentioned, together with the mean outdoor temperature during the same week. The least square analysis and the correlation coefficients are given in Table 1.26.

Again, the weekly means drop when it is warmer outdoors. Also notable is the large difference between the mean and the 95% line, indicating that natatoriums range from humid to very humid.

Nevertheless, as Figure 1.22 underlines, related relative humidity scores far below the 60–70% that wet swimmers need to feel comfortable when drying. The majority in fact have an enclosure, which was not designed to tolerate the comfortable relative humidity needed without suffering from severe moisture damage. However, keeping relative humidity as low as measured, demands intense ventilation, resulting in far too high end energy use for heating.

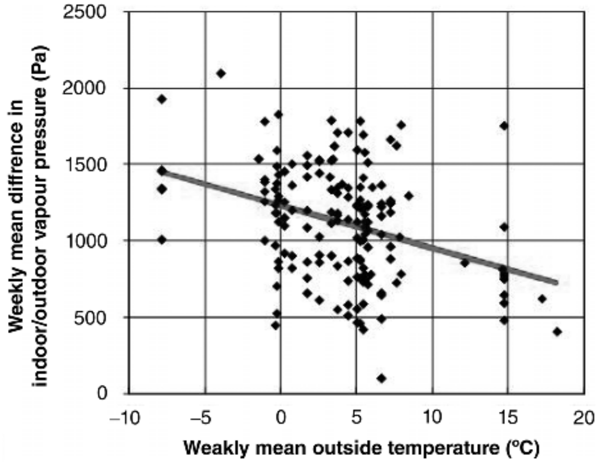

Figure 1.21 Natatoriums: weekly mean indoor/outdoor vapour pressure difference.

Table 1.26 Natatoriums, weekly mean indoor/outdoor vapour pressure difference, relative humidity.

Number of records	Line	$\Delta p_{ie} = a + b\theta_e$		Correlation coefficient r^2	$\phi_i = a + b\theta_i + c\theta_e$			Correlation coefficient r^2
		a, Pa	b, Pa/°C		a %	b %/°C	c %/°C	
162	Mean	1229	–27.7	0.13	125	–2.8	0.36	0.17
	95%	1793	–27.7					

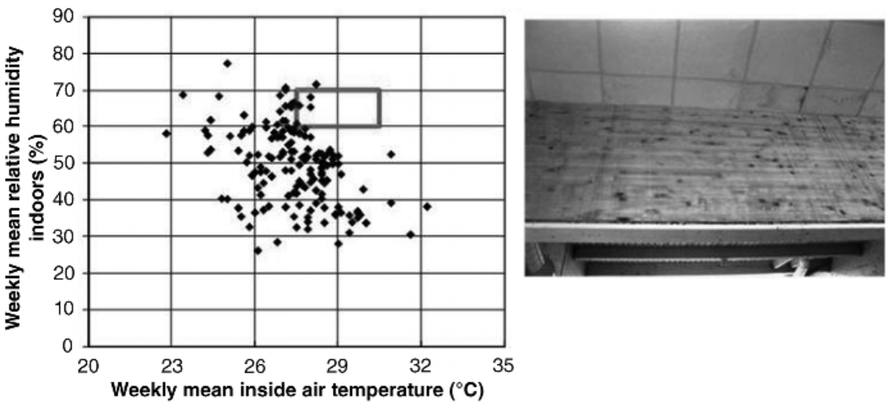

Figure 1.22 Natatoriums: left weekly mean relative humidity indoors in relation to the weekly mean indoor temperature with the rectangle giving the comfort zone, right interstitial condensate dripping off and humidifying the acoustical ceiling in a natatorium.

Table 1.27 Belgium, indoor climate classes ($\overline{\theta}_{e,m}$: gliding monthly mean outdoor temperature).

Indoor climate class		Upper pivot value $\Delta\overline{p}_{ie}$ in Pa $\overline{\theta}_{e,m}$<0? Set 0	Applies to:
1	$\overline{\theta}_{e,m} = 0$ $\overline{\theta}_{e,m} \geq 0$	150 $150 - 8.9\,\overline{\theta}_{e,m}$	All buildings with hardly any vapour release, except for short periods of time (dry storage rooms, sport arenas, garages, etc.)
2	$\overline{\theta}_{e,m} = 0$ $\overline{\theta}_{e,m} \geq 0$	540 $540 - 29\,\overline{\theta}_{e,m}$	Buildings with limited vapour release per m^3 of air volume and appropriate ventilation (offices, schools, shops, large dwellings, apartments)
3	$\overline{\theta}_{e,m} = 0$ $\overline{\theta}_{e,m} \geq 0$	670 $670 - 29\,\overline{\theta}_{e,m}$	Buildings with higher vapour release per m^3 of air volume, but still appropriately ventilated (small dwellings, hospitals, pubs, restaurants)
4		$>670 - 29\,\overline{\theta}_{e,m}$	Buildings with high vapour release per m^3 of air volume (natatoriums, breweries, several industrial complexes, hydrotherapy spaces)

1.3.2.3 Indoor climate classes

The difference in indoor/outdoor vapour pressure is such an important parameter for moisture tolerance that buildings have been grouped into indoor climate classes, using that difference as pivot. Table 1.27 and Figure 1.23 summarize the classes used in Belgium since 1982. The pivot values reflect following situations:

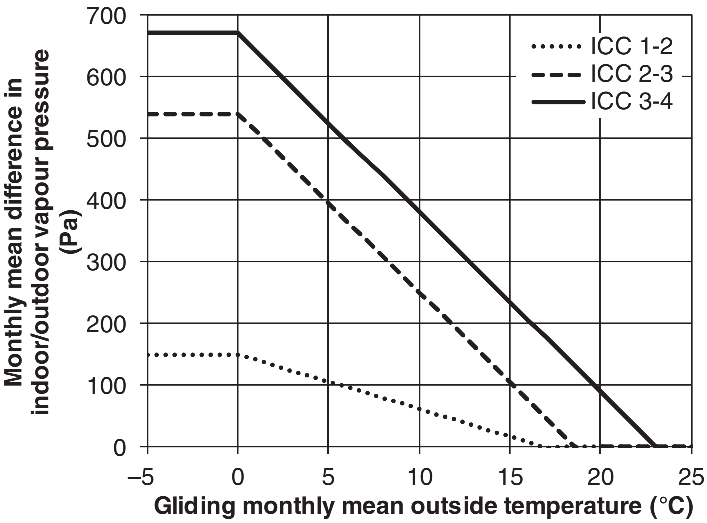

Figure 1.23 Belgium, pivots between the four indoor climate classes.

Table 1.28 Belgium, pivot values between the indoor climate classes recalculated (if $\Delta\overline{p}_{ie} < 0$, set 0).

Indoor climate class		Pivot (Pa)		Pivot (Pa)
1–2	$\overline{\theta}_{e,m} = 0$	87	$\overline{\theta}_{e,m} \geq 0$	$87 - 8.9\,\overline{\theta}_{e,m}$
2–3	$\overline{\theta}_{e,m} = 0$	550	$\overline{\theta}_{e,m} \geq 0$	$550 - 29\,\overline{\theta}_{e,m}$
3–4	$\overline{\theta}_{e,m} = 0$	1030	$\overline{\theta}_{e,m} \geq 0$	$1030 - 29\,\overline{\theta}_{e,m}$

Class 1/2 On a monthly mean basis vapour diffusion does not give interstitial condensation in a continuously shaded, airtight low-slope roof without vapour retarder, composed of non-hygroscopic materials and covered with a vapour tight membrane.

Class 2/3 On a monthly mean basis vapour diffusion does not give accumulating condensate in a north-orientated, non-hygroscopic, airtight wall without vapour retarder at the inside, finished at the outside with a vapour tight cladding.

Class 3/4 On a monthly mean basis vapour diffusion results in accumulating condensate in the roof, used for the class 1/2 pivot but now radiated by the sun.

In indoor climate class 4 a correct heat, air, moisture design of the enclosure is mandatory. In classes 1, 2 and 3, respecting simple design rules suffices. In the 1990s, the pivots were recalculated using transient modelling. The main result was an important shift of the pivot between indoor climate classes 3 and 4, see Table 1.28.

Other countries did the same exercise. Table 1.29 and Figure 1.24 summarize the results produced by Finland and Estonia. They used data collected in 101 dwellings spread over the two countries to come up with pivot values.

A Europe-wide adoption of the concept came with EN ISO 13788, introduced in 2001. The standard grouped buildings not into three or four but into five classes with pivot values as listed in Table 1.30 and shown in Figure 1.25.

Indoor climate classes lose usability as soon as airflow-driven vapour movement intervenes. The concept in fact was developed to evaluate the slow interstitial condensate deposit that diffusion induces, not to judge the much faster built-up convective vapour flow causes. Even indoor climate class 1 buildings may experience problems then.

Table 1.29 Finland and Estonia, indoor climate, pivot values (Δp_{ie}, $\overline{\theta}_{e,w}$: weekly means).

Indoor climate	Difference in indoor/outdoor vapour pressure (Pa)		
	$\overline{\theta}_{e,w} < 5\,°C$	$5 \leq \overline{\theta}_{e,w} \leq 15\,°C$	$\overline{\theta}_{e,w} > 15\,°C$
Low humidity load	540	$540 - 34\,\overline{\theta}_{e,w}$	200
Average humidity load	680	$680 - 41\,\overline{\theta}_{e,w}$	270
High humidity load	810	$810 - 47\,\overline{\theta}_{e,w}$	340

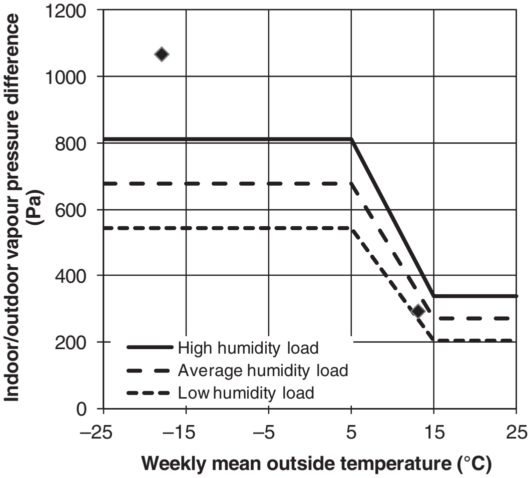

Figure 1.24 Finland and Estonia, indoor climate: differences in indoor/outdoor vapour pressure (the two individual dots represent averages measured in northern Canada).

Table 1.30 EN ISO 13788, indoor climate classes, pivot values.

Indoor climate classes	Annual mean $\Delta\overline{p}_{ie}$(Pa)	
	$\overline{\theta}_{e,m} < 0$	$\overline{\theta}_{e,m} \geq 0$
1–2	270	$270 - 13.5\,\overline{\theta}_{e,m}$
2–3	540	$540 - 27.0\,\overline{\theta}_{e,m}$
3–4	810	$810 - 40.5\,\overline{\theta}_{e,m}$
4–5	1080	$1080 - 54.0\,\overline{\theta}_{e,m}$

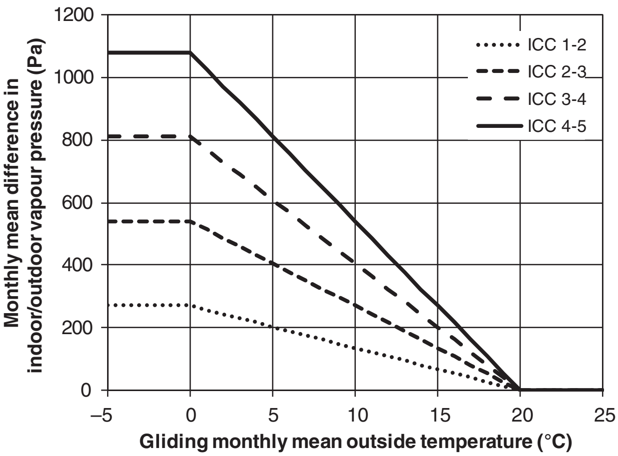

Figure 1.25 The indoor climate classes according to EN ISO 13788.

1.3.3 Indoor/outdoor air pressure differentials

Thermal stack, wind and fans induce air pressure differentials that act as driving force for air infiltration and exfiltration. Wind in turn also favours wind washing, while thermal stack is responsible for indoor air washing and air looping in and across envelope assemblies. Together with the air, non-negligible amounts of water vapour and enthalpy are displaced, causing the thermal transmittances and transient thermal response properties to lose significance; interstitial condensation to become more likely and bulky; end energy consumption to increase; draft complaints to emerge; and sound insulation to degrade.

In winter, thermal stack gives overpressure indoors. In warm weather, that becomes under-pressure when the indoor temperatures drop below that outdoors. Pressure differentials from wind change with wind speed and direction. They also depend on the pressure coefficients and leak distribution over the enclosure and the leak distribution indoors. When, for example, the enclosure is most permeable at the windward side, overpressure indoors will follow with the air leaving at the leeward side and at the sides more or less parallel to the wind. The pressures that forced air heating and mechanical ventilation give differ between spaces; some industrial buildings experience extreme values. In the supply plenum above the HEPA filter ceiling of a clean room laboratory an overpressure up to 150 Pa was measured. An overpressure of 300 Pa was noted in the top-floor of a brewery's hop kiln.

Where wind mainly induces transient differentials and those caused by mechanical ventilation are often negligible, except in very airtight buildings and in some industrial buildings, thermal stack is always active. Pressure differentials induced and related inflows and outflows may reach high values, as Figure 1.26 illustrates for a medium-rise

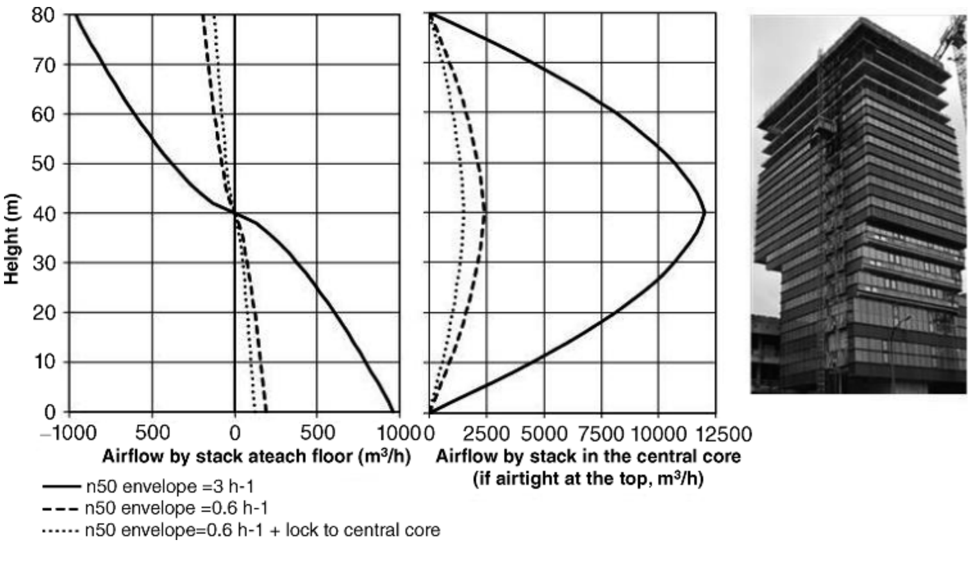

Figure 1.26 Medium-rise office building, air flow caused by thermal stack.

office building. Minimization demands specific measures, such as extreme airtightness of the envelope and an airtight lock around the central core.

Further reading

Anon (1983) *Draft European Passive Solar Handbook,* Section 2 on Climate, CEC.

Flemish government (2006) *Energy Performance Decree,* Text and Addenda (in Dutch).

ASHRAE (2009) *Handbook of Fundamentals*, Chapter 27, Climatic Design Information.

ASHRAE (2013) *Handbook of Fundamentals*, Chapter 27, Climatic Design Information.

Berdahl, P. and Fromberg, R. (1982) The thermal radiance of clear skies. *Solar Energy*, **29**(4), 299–314.

Best, A.C. (1950) The size distribution of rain drops. *Quarterly Journal of the Royal Meteorological Society*, **76**, 16–36.

Blocken, B. (2004) *Wind-driven rain on buildings measurement. Numerical modelling and applications*, PhD thesis, KU Leuven 323 pp.

Blocken, B., Carmeliet, J. and Hens, H. (1999) *Preliminary Results on Estimating Wind Driven Rain Loads on Building Envelopes: A Numerical and Experimental Approach*, Laboratory of Building Physics, KU Leuven, 78 pp.

Blocken, B., Carmeliet, J. and Hens, H. (2000) *On the use of microclimatic data for estimating driving rain on buildings*, Proceedings of the International Building Physics Conference, TU/e, pp. 581–588.

BRE (1971) *An index of exposure to driving rain*, digest 127.

CD with weather data from KU Leuven (1996 –2008) Laboratory of Building Physics.

Cornick, S. and Rousseau, M. (2003) *Understanding the Severity of Climate Loads for Moisture-related Design of Walls*, IRC Building Science Insight, 13 pp.

Cornick, S., Djebbar, R. and Dalgliesh, W. (2003) *Selecting Moisture Reference Years Using a Moisture Index Approach,* IRC Research Paper, 19 pp.

Costrop, D. (1985) *The use of climate data for simulating of thermal systems*, Rapport KU Leuven RD Energie (in Dutch).

Davies, J. and McKay, D. (1982) Estimating solar irradiance and components. *Solar Energy*, **29**(1), 55–64.

Dogniaux, R. (1978) *Recueil des données climatologiques exigentielles pour le calcul des gains solaires dans l'habitat et l'estimation de la consommation de l' énergie pour le chauffage des bâtiments*, KMI (Contract EG) (in French).

EN ISO (2001) 13788. *Hygrothermal performance of building components and building elements – Internal surface temperature to avoid critical surface humidity and interstitial condensation*, calculation method.

EN ISO (2002) 15927. *Hygrothermal performance of buildings*. Calculation and presentation of climatic data.

Geving, S. and Holme, J. (2012) Mean and diurnal indoor air humidity loads in residential buildings. *Journal of Building Physics*, **35**(2), 392–421.

Hartmann, T., Reichel, D. and Richter, W. (2001) Feuchteabgabe in Wohnungen – alles gesagt? *Gesundheits-Ingenieur*, **122**(4) 189–195 (in German).

Hens, H. (1975) *Theoretical and experimental study of the hygrothermal behaviour of building- and insulating materials by interstitial condensation and drying, with application on low-sloped roofs*, doctoraal proefschrift, KU Leuven (in Dutch).

IEA-Annex 14 (1991) *Condensation and Energy*, Sourcebook, ACCO Leuven.

ISO (1980) *Climatologie et industrie du bâtiment*, Rapport, Genève (in French).

Kalamees, T., Vinha, J. and Kurnitski, J. (2006) Indoor humidity loads in lightweight timber-framed detached houses. *Journal of Building Physics*, **29**(3), 219–246.

Kumaran, K. and Sanders, C. (2008) *Boundary conditions and whole building HAM analysis,* Final report IEA-ECBCS Annex 41 Whole Building Heat, Air, Moisture Response, Vol. **3**, ACCO, Leuven, 235 pp.

Künzel, H.M. (2010) Indoor Relative Humidity in Residential Buildings – A Necessary Boundary Condition to Assess the Moisture Performance of Building Envelope Systems.

Künzel, H.M., Zirkelbach, D. and Sedlbauer, K. (2003) *Predicting Indoor Temperature and Humidity Conditions including Hygrothermal Interactions with the Building Envelope*, Proceedings of the First Intenational Conference on Sustainable Energy and Green Architecture, Bangkok, 8–10 October 2003.

Laverge, J., Delgust, M. and Janssens, A. (2014) Moisture in bathrooms and kitchens: the impact of ventilation, *Proceedings of NSB 2014 Lund*, pp. 998–1005 (data stick).

Liddament, M.W. (1986) *Air Infiltration Calculation Techniques*, AIVC.

Poncelet, L. and Martin, H. (1947) *Main characteristics of the Belgian climate*, Verhandelingen van het KMI (in Dutch).

Sanders, C. (1996) *Environmental Conditions,* Final report IEA-ECBCS Annex 24 'Heat, Air and Moisture Transfer in Insulated Envelope Parts', Vol. 2, ACCO, Leuven, 96 pp.

Straube, J. (1998) *Moisture control and enclosure wall systems*, PhD thesis, University of Waterloo (Canada).

Straube, J. and Burnett, E. (2000) *Simplified prediction of driving rain on buildings*, Proceedings of the International Building Physics Conference, TU/e, pp. 375–382.

Ten Wolde, A. and Pilon, C. (2007) The Effect of Indoor Humidity on Water Vapor Release in Homes, *Proceedings of the Buildings X Conference, Clearwater Beach* (CD-ROM).

Uyttenbroeck, J. (1985) *Exterior climate data for energy consumption and load calculations*, Rapport WTCB RD Energie (in Dutch).

Uyttenbroeck, J. and en Carpentier, G. (1985) *Exterior climate data for building physics applications*, Rapport WTCB RD Energie (in Dutch).

Vaes, F. (1984) *Hygrothermal behaviour of lightweight ventilated roofs*, onderzoek IWONL KULeuven TCHN, eindrapport (in Dutch).

Van Mook, F. (2002) *Driving rain on building envelopes*, PhD thesis, TU/e, 198 p.

Wouters, P., L'Heureux, D. and Voordecker, P. (1987) *The wind as parameter in ventilation studies, a short description*, rapport WTCB (in Dutch).

WTCB (1969) *Study of the heat gains by natural illumination of buildings*, Part 1, Solar irradiation, Researchrapport 10 (in Dutch).

WTCB tijdschrift (1982) *Moisture response of building components*, 1 (52 pp.) (in Dutch and French).